IIETA International Information and Engineering Technology Association
Advancing the World of Information and Engineering

Mathematical Modelling of Engineering Problems
Vol. 12, No. 12, December, 2025, pp. 4103-4121
Journal homepage: http://iieta.org/journals/mmep

Application of Kron's Reduction Method to Evaluate Generating Unit Power Variability in the Kron Loss Model Under Economic Dispatch

Arief Goeritno[1,2], Jangkung Raharjo[3,4*], Muhammad Ary Murti[3], Kharisma Bani Adam[3,4]

[1] Student of the Doctoral Program in Electrical Engineering, Telkom University, Bandung 40257, Indonesia
[2] Electrical Engineering Study Program, Bogor Ibn Khaldun University, Bogor City 16164, Indonesia
[3] School of Electrical Engineering, Telkom University, Bandung 40257, Indonesia
[4] Center of Excellence of Sustainable Energy and Climate Change, Telkom University, Bandung 40257, Indonesia

Corresponding Author Email: jangkungraharjo@telkomuniversity.ac.id

https://doi.org/10.18280/mmep.121201

Received: 1 September 2025
Revised: 27 October 2025
Accepted: 4 November 2025
Available online: 31 December 2025

Keywords:
Kron reduction method, economic dispatch, loss coefficients, scalability, network reduction, power variability

ABSTRACT

Kron reduction simplifies power system models by eliminating nodes while preserving electrical equivalence. However, its integration with loss modelling and economic dispatch remains underexplored, particularly the impact of recalculating loss coefficients after each reduction stage. This study develops a feasibility-based Kron reduction framework that integrates a quadratic loss model to evaluate generating unit variability and system efficiency under economic dispatch. Using the IEEE-30 bus benchmark, peripheral buses were eliminated based on a composite peripherality index combining electrical connectivity and load participation. For each reduced network, B-coefficients are recalculated, and economic dispatch is performed using quadratic cost functions and the fmincon nonlinear optimizer in MATLAB. Voltage deviations remained below 0.5%, complying with IEEE Std 399-1997 limits. Generators near load centers showed higher variability due to stronger electrical coupling, while peripheral units remained stable. Runtime efficiency improved by up to 40% across reduction stages, consistent with the $O(n^3)$ computational trend. The proposed method maintains accuracy and operational feasibility, offering a transparent and scalable approach suitable for integration into real-time supervisory control and data acquisition (SCADA) and energy management systems (EMS) environments.

1. INTRODUCTION

Network reduction techniques, particularly Kron's reduction, are widely employed in power system analysis to simplify large-scale networks while retaining the essential electrical characteristics of the retained buses. This process is critical in real-time applications such as supervisory control and data acquisition (SCADA) and energy management systems (EMS), where computational efficiency directly impacts operational decision-making. Recent advances have demonstrated that optimized implementations of Kron's reduction can significantly enhance dispatching efficiency while preserving network accuracy [1]. In parallel, complementary strategies using intelligent algorithms have also been applied to improve operational efficiency in distribution networks, highlighting the broader relevance of reduction and optimization methods for modern power system management [2]. Recent studies have shown that applying Kron's Reduction Methods (KRM) to IEEE benchmark systems can yield substantial reductions in computational complexity without significantly degrading accuracy in voltage profiles, power flows, and loss calculations [3-5]. The IEEE-30 bus system, a standard test network for economic dispatch and load flow studies, offers a practical scale for evaluating reduction strategies before their application to larger transmission networks [6, 7].

Despite numerous applications of KRM, there remains limited research on progressive multi-stage reduction strategies that assess the impact of eliminating specific load buses on system performance under economic dispatch conditions. Most prior work has focused either on single-step reductions or on reduced models for steady-state power flow without evaluating generator output variability, performance benchmarking metrics, or operational compatibility with EMS [8]. Although KRM has been applied in sequential elimination of PQ (load) buses to assess impacts on voltage profiles and state estimation accuracy [9], and in scalable simplifications of multiple IEEE test systems showing preserved direct current (DC) power flow equivalence [10], no study has yet combined these elements into a progressive multi-stage reduction framework under economic dispatch conditions—one that assesses generator dispatch variability, performance benchmarking metrics, operational EMS compatibility, and scalability—especially when quadratic loss models are integrated into the process. Additionally, recent literature lacks comprehensive evaluations linking bus elimination sequences to scalability assessments across varying system sizes. This gap creates uncertainty in determining optimal bus elimination orders that balance accuracy, computational speed, and operational feasibility—particularly when integrating quadratic loss models into the dispatch process [3].

Recent advancements in power system modeling have increasingly focused on reducing computational complexity without compromising accuracy, especially in the context of real-time applications. The KRM, first introduced in the mid-20th century, has regained attention in modern power engineering research due to its capability to simplify network matrices while retaining key electrical characteristics [3, 11]. This technique is now being re-examined in the era of large-scale renewable integration, microgrids, and dynamic operational environments. Modern studies leverage improved computational tools and data availability to apply KRM not only for steady-state analysis but also for stability studies, contingency analysis, and optimization-based applications such as economic dispatch [11-13]. The IEEE-30 bus system is widely adopted as a benchmark for validating network reduction algorithms due to its balance between realistic complexity and modelling tractability, e.g., load-ability and voltage stability studies [14, 15]. Contemporary research also applies variants of KRM, e.g., structure-preserving and computational-efficient KRM approaches across IEEE test systems, demonstrating preserved power flow results, loss estimations, and runtime gains [11, 16]. However, most studies still limit their evaluation to single-step reductions, primarily focusing on voltage magnitude accuracy and minimizing power loss deviations, rather than exploring multi-stage strategies [11, 16].

Emerging approaches now explore hybrid reduction techniques, notably combining KRM with graph-theoretic heuristics and optimization strategies to enhance reduction quality and adaptability across diverse network topologies. For instance, Grudzien et al. [11] proposed an iterative, topology-aware Kron reduction framework that aggregates coherent substructures like tree and mesh components, thereby preserving power-flow equivalence while simplifying large-scale networks. Complementing this, Chevalier and Almassalkhi's [3] Opti-KRON method embeds a mixed-integer linear programming (MILP) approach constrained by graph Laplacian structure to compute optimal node eliminations—yielding significant model reduction with minimal voltage deviation in seconds [3]. Despite these advancements, there remains a notable gap: The literature has yet to offer comprehensive multi-stage reduction studies that evaluate the operational implications of progressive bus elimination sequences —particularly in terms of generator dispatch variability, performance benchmarking, and real-time compatibility with SCADA/EMS systems. Most existing works, including the above, focus primarily on the accuracy of static power flow results or runtime improvements without assessing dynamic dispatch outcomes or system-level operational requirements. Furthermore, scalability assessments—in particular, how reduction strategies perform when transitioning from medium-sized systems like the IEEE-30 bus to much larger, real-world networks—remain insufficiently explored. Recent work by Mokhtari et al. [17] addresses this by extending Opti-KRON with community detection (CD)-based decomposition, enabling scalable reductions across large systems, e.g., IEEE RTS-96 and the 2,383-bus Polish grid, with reductions of 80–95% in node count while retaining performance fidelity. Addressing these gaps—through structured multi-stage elimination protocols, operational benchmarking, and cross-system scalability studies—is essential to validate KRM's robustness under real-world constraints and to inform its integration into operational planning and control strategies in modern power systems.

Modern power systems are becoming increasingly complex due to the integration of renewable energy sources, e.g., solar and wind, proliferation of distributed generation, and evolving operational demands such as demand response and microgrid interactions [11, 12]. These developments place growing pressure on computational efficiency for real-time tasks including monitoring, optimization, economic dispatch, and contingency analysis [3]. Kron's reduction method offers a mathematically principled means to simplify large-scale network models by eliminating noncritical buses while preserving electrical equivalence at the retained nodes [8, 11]. Yet, the operational effects of using KRM in economic dispatch contexts, especially under progressive (multi-stage) reduction schemes, remain under-investigated. While static simplification can significantly reduce computation time, it may also introduce deviations in voltage magnitude, power loss estimation, and generator output—parameters critical for decision-making in SCADA/EMS [3, 11]. Moreover, dynamic phenomena underscore that disturbances originating in eliminated nodes can reverberate through the network affecting retained-bus behaviour—highlighting that reduced models must be validated not just for steady-state accuracy but also for dynamic fidelity in real-time operational contexts [12]. Despite these motivations, most existing studies remain limited to single-step, static reductions, and do not systematically examine generator dispatch variability, benchmark performance metrics, or scalability from medium networks, e.g., IEEE-30 bus to large-scale grids. Furthermore, recent findings on dynamic phenomena indicate that disturbances in reduced nodes can significantly influence the behaviour of retained nodes, underlining the importance of accounting for such impacts in real-time applications [18].

Therefore, the core problem addressed in this study is how to apply KRM in multiple stages to the IEEE-30 bus system while ensuring that the reduced models preserve the essential electrical and operational characteristics needed for reliable real-time decision-making in EMS and SCADA environments [19, 20]. The research seeks to evaluate the trade-off between computational efficiency and accuracy, assess generator output variability, and verify compatibility with operational control environments. A schematic diagram of problem formulation is shown in Figure 1. Based on Figure 1, it can be explained that a problem formulation schematic showing the relationship between the full model, reduction process, and evaluation targets.

The research pursues five main objectives:

(i) to analyze the impact of KRM on medium-scale power systems;

(ii) to evaluate generating unit power variability under a quadratic loss model in reduced-order networks;

(iii) to benchmark key performance metrics such as total power loss deviation, Voltage Root Mean Square Error (V-RMSE), and simulation runtime;

(iv) to assess operational compatibility of reduced models with economic dispatch frameworks; and

(v) to evaluate the scalability of the approach. The study contributes by performing staged KRM on the IEEE-30 bus system—a stepwise node elimination approach not commonly found in previous works. It offers detailed comparisons between full and reduced models by examining generator outputs and preserved power flows across each reduction stage, thereby validating both operational fidelity and reduction efficacy [1]. This comprehensive evaluation provides power system engineers with quantitative insights into the trade-offs between computational efficiency and accuracy, guiding informed adoption of network reduction in practice [17]. This article is structured to provide a coherent narrative from problem identification to the presentation of results and implications. Section 1 introduces the research background and gap analysis, reviews the state-of-the-art in Kron's reduction techniques and related network simplification methods, problem formulation, research objectives, contribution opportunity, and novelty potential. Section 2 frames the study within existing literature reviews. Section 3 presents the methodology, detailing the framework, materials and tools, and reduction procedures and research methods. Section 4 discusses the results and analysis based on five objectives. Section 5 outlines the conclusions, contributions, novelty, and directions for future work. The last Section lists the references following the citation guidelines of a journal, ensuring traceability, and reproducibility.

The key contributions of this research are:

(i) introducing a structured multi-stage bus elimination sequence (bus-26, bus-30, and bus-29) for the IEEE-30 bus system;

(ii) benchmarking V-RMSE, power loss deviation, and computation time at each stage;

(iii) validating operational compatibility with economic dispatch incorporating quadratic loss models. The proposed approach demonstrates applicability for scaling KRM to medium and larger networks while preserving operational fidelity [2, 17]. This study's novelty lies in its unified evaluation of KRM across multiple operational objectives in a staged reduction sequence rather than a single reduction step. Unlike most existing works focusing only on load flow accuracy, this research integrates assessments of generator output variability, operational compatibility, and scalability [1]. Using the IEEE-30 bus system as a reference model bridges theoretical reduction strategies and their real-time SCADA and/or EMS applications—its established use in software-based substation models, e.g., in ETAP enables more adaptive and efficient planning for medium- and larger-scale power systems [21].

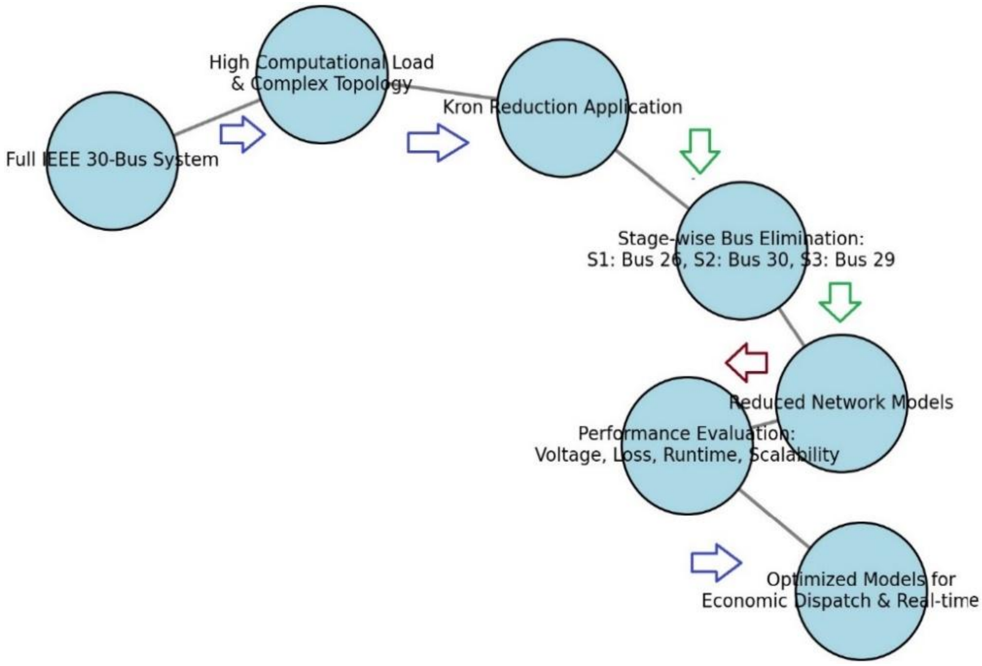

Figure 1. A schematic diagram of problem formulation

2. LITERATURE REVIEW

The contents of this literature review chapter include three main things that are closely related to the title of the article, namely (i) KRM [22] and its application are historical background, mathematical basis, modern adaptations, and power system uses [17, 23-25]; (ii) generating unit power variabilities in the Kron's Loss Model (KLM) [26] are quadratic loss model [27], effects of network reduction [23-25], and sensitivity factors [28]; and (iii) economic dispatch phenomena are fundamentals [26, 27, 29], integration with network models, the role of reduced networks, and recent improvements are particularly relevant in the context of the application [30] of KRM [22] to evaluate generating unit power variability in the KLM [31] under economic dispatch [27]. These three areas form the theoretical and empirical backbone for evaluating the objectives in this study.

2.1 KRM and its application

Kron's reduction method, first introduced by Gabriel Kron in 1939 [22], was originally developed to simplify electrical network equations by eliminating selected internal nodes. Over time, the method evolved through structured matrix transformations and became a fundamental tool in control theory and power system engineering [23-25, 32]. At its core, Kron's reduction is a mathematical technique that simplifies the network admittance matrix (Y-bus) by applying the Schur complement. This technique preserves the electrical characteristics of retained nodes while reducing the system size [23-25]. It is particularly valuable for minimizing computational complexity in power system studies, especially when analysing the interactions between principal buses. In practical applications, it is widely used to remove non-essential nodes such as radial or unloaded buses, thus streamlining the analysis without significantly affecting system accuracy [1]. Kron Reduction as a source of variability, i.e., (i) KRM simplifies the system by eliminating nodes and redistributing admittances [25], (ii) This changes impedance pathways, which can affect: loss coefficients (B-coefficients) in the quadratic loss model and participation factors, i.e., how each generator contributes to balancing demand [18]; and (iii) If not carefully staged, KRM could distort dispatch patterns and make the reduced model unrepresentative.

The KRM has been extensively applied in modern power system analysis, notably in model order reduction [23-25], short-circuit studies [8], steady-state assessments [9], and dynamic simulations [3, 8]. When applied to the bus admittance matrix, the Schur complement ensures that voltages at retained buses remain equivalent to those in the full model, making KRM ideal for system simplification without compromising critical accuracy [23-25]. In contemporary research, KRM supports applications [3, 9] like contingency analysis, optimal power flow (OPF), and state estimation [27, 33, 34], where computational efficiency is essential [33, 35]. Moreover, the method's role has expanded to accommodate medium- or large-scale grids that integrate renewable energy sources, which require real-time responsiveness and high-fidelity modelling [3, 9, 23-25]. By maintaining operational characteristics while reducing model dimensionality, Kron's reduction provides practical benefits in creating accurate equivalents for contingency scenarios, economic dispatch simulations, and stability studies [23-25].

Recent studies have extended its application to large-scale grids, integrating renewable generation and examining real-time feasibility in control environments [1, 3, 9]. Mathematically, KRM is a Schur complement on the bus-admittance matrix (Y) [23-25]. Let the retained buses be B (all buses except bus-n), and the eliminated set be $I = n$. Partition Y as shown in Eq. (1).

$$\boldsymbol{Y} = \begin{bmatrix} \boldsymbol{Y_{BB}} & \boldsymbol{Y_{BI}} \\ \boldsymbol{Y_{IB}} & \boldsymbol{Y_{II}} \end{bmatrix} \tag{1}$$

with $\boldsymbol{Y_{II}} = [\boldsymbol{Y_{n,n}}]$, $\boldsymbol{Y_{BI}} = [\boldsymbol{Y_{b,n}}]$, and $\boldsymbol{Y_{IB}} = [\boldsymbol{Y_{n,b}}]^{\boldsymbol{T}}$.

The reduce matrix is shown in Eq. (2).

$$\begin{aligned} \boldsymbol{Y^{reduction}} &= \boldsymbol{Y_{BB}} - \boldsymbol{Y_{BI}} \cdot \boldsymbol{Y_{II}}^{-1} \cdot \boldsymbol{Y_{IB}} \\ &= \boldsymbol{Y_{BB}} - \frac{1}{\boldsymbol{Y_{II}}} \cdot \boldsymbol{Y_{BI}} \cdot \boldsymbol{Y_{IB}} \end{aligned} \tag{2}$$

For the stage when reduction is carried out on bus-26 which is only adjacent to bus-25, then only entries that "touch" neighbours of bus-26 change. In the stage where bus-26 (a dead-end node connected only to bus-25) is eliminated via Kron reduction, only matrix entries associated with bus-25, i.e., the neighbours of bus-26—are updated in the Y-bus. This behaviour follows directly from the nature of the Schur complement in Kron reduction, where perturbations affect only adjacent nodes [23-25]. If $\aleph(26)$ is the set of buses directly connected to 26, then for any $i, j \in \aleph(26)$ (possibly $i = j$):

#Off-diagonal (create or update an equivalent link) is shown in Eq. (3).

$$\boldsymbol{Y_{ij}^{reduction}} = \boldsymbol{Y_{ij}} - \frac{1}{\boldsymbol{Y_{26,26}}} \cdot \boldsymbol{Y_{i,26}} \cdot \boldsymbol{Y_{26,j}},\ \boldsymbol{i \neq j} \tag{3}$$

#Diagonal of a neighbour (self-admittance update) is shown in Eq. (4).

$$\boldsymbol{Y_{ii}^{reduction}} = \boldsymbol{Y_{ii}} - \frac{\boldsymbol{1}}{\boldsymbol{Y_{26,26}}} \cdot \boldsymbol{Y_{i,26}} \cdot \boldsymbol{Y_{26,i}} \tag{4}$$

All other entries remain the same.

$\boldsymbol{Y_{26,26}}$ is the self-admittance at bus-26 (sum of incident branch admittances plus shunt at bus-26). $\boldsymbol{Y_{i,26}} = \boldsymbol{Y_{26,i}} = -\boldsymbol{y_{i,26}}$ for a simple series branch $\boldsymbol{y_{i,26}} = \boldsymbol{1/r_{i,26}} + \boldsymbol{j} * \boldsymbol{x_{i,26}}$.

In the standard IEEE-30 bus system, bus-26 is a radial node, connected exclusively to bus-25—this isolated linkage underlines its role as a dead-end bus in system topology (i.e., only one incident branch in the line data), then $\aleph(26) = \{25\}$ [23-25]. There is no new tie created because there's only a single neighbour, so that there are two explanations:

#i) update only the 25–25 diagonal is used Eq. (4), so that Eq. (4) becomes Eq. (5).

$$\boldsymbol{Y_{25,25}^{reduction}} = \boldsymbol{Y_{25,25}} - \frac{\boldsymbol{1}}{\boldsymbol{Y_{26,26}}} \cdot \boldsymbol{Y_{25,26}} \cdot \boldsymbol{Y_{26,25}} \tag{5}$$

#ii) all other entries are unchanged.

In the IEEE-30 bus test system, bus-30 is connected to both bus-27 and bus-29, reflecting its mesh configuration within the network topology [23-25]. This detail is clearly documented in single-line diagrams and contingency analyses, which note that "bus-30 (2nd weakest bus) has got connections to both bus-27 and bus-29" [36, 37], so that $\aleph(30) = \{27{,}29\}$, and then we both update diagonals and create a new mutual admittance between 27 and 29 are shown in Eqs. (6)-(8) [23-25].

$$\boldsymbol{Y_{27,27}^{reduction}} = \boldsymbol{Y_{27,27}} - \frac{\boldsymbol{1}}{\boldsymbol{Y_{30,30}}} \cdot \boldsymbol{Y_{27,30}} \cdot \boldsymbol{Y_{30,27}} \tag{6}$$

$$\boldsymbol{Y_{29,29}^{reduction}} = \boldsymbol{Y_{29,29}} - \frac{\boldsymbol{1}}{\boldsymbol{Y_{30,30}}} \cdot \boldsymbol{Y_{29,30}} \cdot \boldsymbol{Y_{30,29}} \tag{7}$$

$$\boldsymbol{Y_{27,29}^{reduction}} = \boldsymbol{Y_{27,29}} - \frac{\boldsymbol{1}}{\boldsymbol{Y_{30,30}}} \cdot \boldsymbol{Y_{27,30}} \cdot \boldsymbol{Y_{30,29}} \tag{8}$$

Eq. (8) is the new direct coupling.

The method has been widely applied in power system analysis for tasks such as model order reduction [1, 38, 39], short-circuit studies [40], and dynamic simulations [3, 9]. Applying the Schur complement, the reduced Y-bus matrix maintains equivalent voltages at retained buses, making it suitable for applications where network simplification is required without compromising accuracy [1, 38, 40]. In power system applications, the Kron reduction method has been used for network equivalencing to facilitate contingency analysis [38], optimal dispatch [3, 9, 29], and state estimation [34, 39]. Recent studies have extended its application to medium- or large-scale grids, integrating renewable generation [1] and examining real-time feasibility in control environments [3, 9, 29]. These works highlight the importance of balancing computational efficiency with fidelity to the original system [3, 9]. The KRM in the context of transmission network studies, it offers a means to reduce the dimensionality of system models while preserving the electrical characteristics relevant to the retained buses [1, 32]. Recent studies have demonstrated its utility in creating equivalent networks for contingency analysis [38], optimal power flow [39], and dynamic stability studies [39].

However, the majority of these studies focus on one-step reduction approaches without systematically evaluating multi-stage elimination sequences [38, 41]. In parallel, researchers have explored advanced network reduction techniques that incorporate machine learning and adaptive algorithms for better retention of operational characteristics [3]. While these methods have shown promise in large-scale simulations, they often come with higher computational overhead, making them less suitable for real-time applications [39]. Moreover, traditional Kron's reduction continues to be favoured in practice due to its analytical transparency and ease of implementation [1, 3, 9]. The gap remains in understanding how stage-wise bus elimination affects operational performance metrics such as V-RMSE, loss deviations, and generator dispatch variability [41]. Existing literature also indicates a growing interest in integrating network reduction with real-time control environments such as SCADA and EMS [42, 43]. Ensuring operational compatibility after reduction is critical, particularly for systems incorporating renewable generation and complex load dynamics [38]. Despite this, comprehensive frameworks that assess reduction impact across multiple operational objectives, i.e., voltage profile accuracy, generator variability, runtime efficiency, and scalability are sparse. This study addresses that gap by implementing a multi-stage reduction sequence and evaluating it against these criteria using the IEEE-30 bus system [36, 37].

2.2 Generating unit power variability in the KLM

The concept of generating unit power variability in the KLM addresses how network reduction influences the allocation and fluctuation of generation outputs within power systems [38]. Kron's reduction method is widely applied to simplify large-scale systems by eliminating certain buses, thereby reducing the size of admittance and impedance matrices while preserving the electrical behaviour between retained buses [1]. However, such reduction can impact the accuracy of system parameters, particularly when assessing active and reactive power generation variability at individual generator buses [23-25]. In the context of the KLM, which models real power losses as a quadratic function of nodal power injections, the reduction process can alter the loss coefficients and the distribution of system losses among generators [27]. The variability of generator outputs becomes an important performance metric, as it reflects the sensitivity of dispatch schedules to changes introduced by the reduced-order network representation. This is particularly critical in economic dispatch applications, where generation schedules are optimized to minimize operational costs while meeting demand and technical constraints [44]. Studies have shown that while Kron reduction can significantly reduce computational burden, it must be applied carefully to avoid large deviations in generator dispatch patterns [3]. The impact depends on the location of eliminated buses, the degree of electrical connectivity, and the weighting of loss coefficients in the dispatch optimization [45]. Sensitivity analyses are often employed to evaluate generator output variability under different reduction scenarios, ensuring that reduced models remain operationally compatible with full-scale systems.

The quadratic loss model, which expresses transmission losses as a quadratic function of generator outputs, has been a fundamental element in economic dispatch problems. Loss coefficients (*a*, *b*, *c*) are derived from network parameters and used to compute total system losses under different dispatch scenarios [46]. When combined with Kron reduction, the quadratic loss model enables evaluation of how network simplification impacts dispatch decisions and system-level losses [27]. Performance benchmarking in reduced-order models often involves metrics such as voltage RMSE, power loss deviation, and simulation runtime [47]. Studies have shown that network reduction can reduce computational time significantly. As demonstrated in adaptive model reduction studies for large test systems, network reduction can significantly reduce simulation time while maintaining and preserving acceptable accuracy [48]. Scalability remains a key focus, with research suggesting that methods like Kron reduction can be adapted for high-bus-count systems with minimal accuracy degradation [17]. The KLM based on a quadratic power loss equation is implemented on both the full and reduced-order networks. This enables the evaluation of generating unit power variability by quantifying changes in generation dispatch profiles, total system losses, and nodal power injections [27]. Together these sources support a comparative study between full vs. reduced models across (i) voltage deviations, (ii) generator-output differences, (iii) benchmarking metrics (loss deviation, voltage error, runtime), (iv) operational compatibility with ED/real-time control constraints, and (v) scalability to large systems.

2.3 Economic or optimal dispatch: A mathematical perspective

Economic dispatch (ED) is a fundamental optimization problem in power system operation, aiming to determine the optimal generation levels for all committed generating units so as to meet the total load demand at the lowest possible operating cost, subject to system and unit constraints [27, 49]. The ED problem is formulated based on the principle of equal incremental costs of all operating units, adjusted for transmission losses, ensuring that generation is allocated efficiently across the system. Based on mathematically, the basic ED problem can be expressed as the minimization of the total generation cost [50-53].

Minimize: It is shown in Eq. (9).

$$\boldsymbol{C_{total} = \sum C_i\left(P_{gi}\right) \quad \text{for } i = 1 \; to \; N_g} \tag{9}$$

where, $\boldsymbol{C_i(P_{gi})}$ is the cost function of the i-th generator, usually modeled as a quadratic function is shown in Eq. (10).

$$\boldsymbol{C_i\left(P_{gi}\right) = a_i + b_i \cdot P_{gi} + c_i \cdot {P_{gi}}^2} \tag{10}$$

Here, $\boldsymbol{P_{gi}}$ is the power output of the i-th generating unit, and $\boldsymbol{a_i}$, $\boldsymbol{b_i}$, and $\boldsymbol{c_i}$ are cost coefficients.

The ED problem is subject to two main types of constraints, i.e., power balance constraint and generator operating limits. Both constraints are shown in formulas (11) and (12).

$$\boldsymbol{\sum P_{gi} = P_{demand} + P_{losses}} \tag{11}$$

where, $\boldsymbol{P_{demand}}$ is the total system demand and $\boldsymbol{P_{losses}}$ is the total transmission loss.

$$\boldsymbol{P_{gi_{min.}} \leq P_{gi} \leq P_{gi_{max.}}} \tag{12}$$

which ensures that each generating unit operates within its technical limits. Incorporating transmission losses into ED requires the use of loss coefficients, often represented through the KLM. In this approach, total transmission loss is expressed as a quadratic function of generator outputs is shown in Eq. (13) [27, 31, 50, 51].

$$\boldsymbol{P_{losses}} = \sum \left(\sum \boldsymbol{P_{gi}} \cdot \boldsymbol{B_{ij}} \cdot \boldsymbol{P_{gj}} + \sum \boldsymbol{B_{0i}} \cdot \boldsymbol{P_{gi}} + \boldsymbol{B_{00}} \right) \quad (13)$$

where, $\boldsymbol{B_{ij}}$, $\boldsymbol{B_{0i}}$, and $\boldsymbol{B_{00}}$ are loss coefficients obtained from system data. This model enhances realism in the ED formulation by accounting for internal system losses, which are crucial in operational planning [31, 54]. The KLM thus directly couples with the ED formulation by modifying the power balance equation, affecting the optimal generator outputs.

Various methods can be applied to solve the ED problem, including classical approaches such as the Lambda-iteration method for systems without losses, and iterative Newton-Raphson or gradient-based methods when losses are considered. In recent research, metaheuristic algorithms such as Genetic Algorithms (GA), Particle Swarm Optimization (PSO), and Differential Evolution (DE) have also been successfully applied to ED problems, particularly for complex, nonlinear, or non-convex cost functions [55]. The economic dispatch problem uses an objective function to minimize total generation cost, subject to system power balance constraints, generator operating limits, and network loss equations [56-58]. This is solved using numerical optimization methods, applied consistently to both the full and reduced networks, allowing a fair comparison of dispatch results and operational efficiency [59]. In the economic dispatch study (which ends with OPF), KRM is an aid to reduce model complexity so that the optimization algorithm can more easily find the minimum power loss solution while still considering the network's technical constraints [3].

3. METHODOLOGY

The research methodology for the study is structured to systematically analyse how network reduction influences generator performance, power loss modelling, and economic dispatch efficiency in a realistic power system environment. The study begins with the development of a full IEEE-30 bus system model as the baseline reference [60-62]. This model incorporates detailed bus data, line parameters, generator characteristics, and load profiles, enabling accurate representation of the network's operational state. The KRM is then applied in a staged manner to eliminate selected PQ buses while preserving the electrical equivalence at the retained buses. This step involves the iterative computation of reduced-order admittance (Y-bus) matrices using matrix partitioning techniques, ensuring that voltage relationships and system impedances remain consistent with the original network [35, 63]. Validation of the reduction process is achieved by staged evaluation after each bus elimination step, ensuring that accuracy thresholds for voltage deviation and power loss difference remain within acceptable engineering limits [20]. The methodology also incorporates visualization techniques, such as topology diagrams, performance curves, and comparative bar charts, to facilitate intuitive interpretation of results [64]. Integrating KRM with economic dispatch analysis and loss modelling, this research methodology provides a structured framework to determine the trade-offs between computational efficiency and operational fidelity, thereby supporting informed decisions in power system operation and planning [26].

3.1 Research framework

The methodological framework integrates analytical modelling, numerical simulations, and comparative performance evaluation [9, 20]. This study employs a structured methodological framework designed to evaluate the technical, operational, and computational implications of applying Kron's reduction method [1] to the IEEE-30 bus system. The methodology aligns directly with the five specific objectives, ensuring that each stage of the research produces results relevant to scalability, generator variability, performance benchmarking, operational compatibility, and applicability to medium- or large-systems [26]. This study employs a quantitative-experimental research design to analyze the impact of Kron Reduction on power system models in the context of economic dispatch [3]. The IEEE-30 bus system is used as a benchmark case [38]. The methodology involves applying step-by-step network reduction techniques, evaluating power system metrics, and benchmarking between the original and reduced models [3, 38]. The overall approach aims to quantify performance trade-offs and assess the operational feasibility of reduced-order models for real-time dispatch applications [3, 65].

In this study, a unified research framework is developed to address five interrelated objectives:

(i) analyzing the impact of KRM on voltage profile preservation,

(ii) evaluating generator output variability under quadratic loss modeling,

(iii) benchmarking performance metrics of reduced versus full networks,

(iv) assessing operational compatibility with economic dispatch frameworks,

(v) evaluating scalability for larger system applications. These objectives reflect core challenges identified in recent literature on power system reduction and dispatch optimization.

Prior studies have demonstrated that KRM can effectively preserve voltage characteristics and network behaviour in reduced-order models [1], that quadratic loss formulations play a central role in capturing generator variability within economic dispatch [26], and that systematic frameworks such as Opti-KRON are essential for benchmarking accuracy while ensuring scalability and operational feasibility [3]. Building on these foundations, the present work integrates all five objectives into a staged evaluation framework for the IEEE-30 bus system.

The research framework integrates network reduction theory, economic dispatch principles, and performance benchmarking into a unified evaluation process [3, 20]. Kron's reduction serves as the core analytical technique [3, 38], reducing the dimensionality of the bus system while preserving electrical equivalence for retained buses [20]. The framework ensures that each objective is addressed systematically [1]. Methodological framework for staged KRM applied to the IEEE-30 bus system in this study is designed to systematically evaluate the performance of Kron's reduction method applied in a multi-stage sequence to the IEEE-30 bus system [3, 38].

As part of this study, we designed a three-stage reduction (bus-26, bus-30, and bus-29 are removed). The framework encompasses three sequential reduction stages, e.g., Stage 1 (S1, removal of bus-26), Stage 2 (S2, removal of bus-30), and Stage 3 (S3, removal of bus-29) This staged approach was evaluated across multiple objectives, following established practices in the literature [1, 3, 9]. Then for the conceptual backbone—multi-objective evaluation, benchmarking, alignment with established methods—use the citations above to demonstrate methodological rigor and comparability. Each stage is evaluated against five research objectives, i.e., voltage profile comparison, generator output variability, performance benchmarking, operational compatibility, and scalability assessment. This multi-objective evaluation is intended to reveal trade-offs between computational efficiency [9] and the preservation of operational accuracy [3]. The framework is aligned with established power system simulation practices, ensuring comparability with existing studies in the literature [1].

3.2 Materials and tools of research

The study utilizes the IEEE-30 bus test system as the reference network, which includes 6 generator buses, 24 load buses, and 41 transmission lines. The network data (bus, branch, and generator parameters) are obtained from the IEEE test case archive to ensure standardization and reproducibility [61-63]. A single line diagram of IEEE-30 bus test system is shown in Figure 2.

Based on Figure 2, it can be explained that the IEEE-30 bus network consists of 30 buses interconnected by 41 transmission lines, six generator buses located at buses of 1, 2, 13, 22, 23, and 27, and one slack bus at bus 1. It also contains 24 load buses and four tap-changing transformers. Shunt capacitors are installed at selected buses to enhance voltage stability.

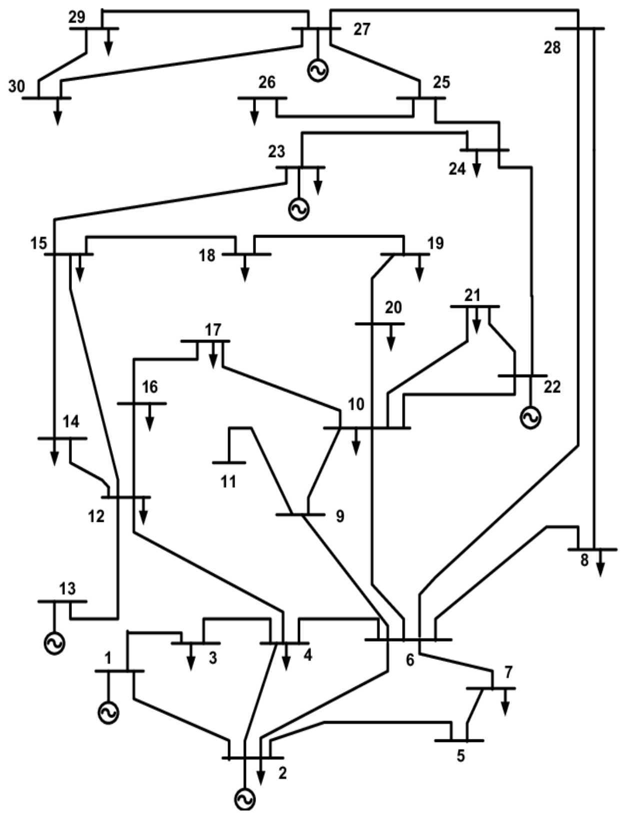

Figure 2. A single line diagram of IEEE-30 bus test system

Table 1. The specific criteria for each bus in the IEEE-30 bus system

Bus No.	Bus Type	Function	Role	Criteria
1	Slack	Reference Generator	High voltage control importance	Retained
2	PV	Generator	Moderate load & generation	Retained
3	PQ	Load	Central load	Retained
4	PQ	Load	High connectivity	Retained
5	PQ	Load	Moderate load	Retained
6	PQ	Load	Moderate load	Retained
7	PQ	Load	Proximity to main corridor	Retained
8	PQ	Load	Local load	Retained
9	PQ	Load	Central network	Retained
10	PQ	Load	Moderate load	Retained
11	PQ	Load	Low load, weak tie	Retained
12	PQ	Load	Industrial load	Retained
13	PV	Generator	Major generator	Retained
14	PQ	Load	Feeder to local load	Retained
15	PQ	Load	Feeder to local load	Retained
16	PQ	Load	Feeder to local load	Retained
17	PQ	Load	Moderate load	Retained
18	PQ	Load	Local load	Retained
19	PQ	Load	Peripheral	Retained
20	PQ	Load	Moderate load	Retained
21	PQ	Load	Peripheral	Retained
22	PV	Generator	Generation support	Retained
23	PV	Generator	Generation support	Retained
24	PQ	Load	Peripheral	Retained
25	PQ	Load	Peripheral	Retained
26	PQ	Load	Low load, weak tie	Reduced 1
27	PV	Generator	Generation support	Retained
28	PQ	Load	Peripheral	Retained
29	PQ	Load	Redundant supply	Reduced 3
30	PQ	Load	Peripheral, low load	Reduced 2

The IEEE 30-bus system was selected as the benchmark case due to its long-standing use in power system optimization, load flow, and reduction studies Wood et al. [27], Alsac and Stott [59]; Liu et al. [4]. It offers a well-balanced representation of generation, transmission, and load characteristics while remaining computationally tractable for detailed validation of staged reduction and loss modeling approaches. The simulation environment is developed in Matrix Laboratory (MATLAB) version R2023b [66], leveraging its Power System Analysis Toolbox (PSAT) for load flow calculations [67], Kron reduction implementation, and data visualization were conducted using established methods and software [9, 25, 68]. It introduces PSAT as an open-source MATLAB/Simulink-based software package. It covers features such as load flow, optimal power flow, time-domain simulation, continuation power flow, and interfaces with MATLAB for visualization with relevant that often cited when someone want to justify or document the use of PSAT as a software environment for simulation, algorithm testing, or visualization [67]. The computational platform consists of a workstation with an Intel Core i7-12700K Central Processing Unit (CPU), 32 gigabyte (GB) Random Access Memory (RAM), and Windows 11 Pro 64-bit operating system (OS). The primary software tools used include MATLAB for algorithm execution, Microsoft Excel for intermediate data handling, and Microsoft Word for report preparation. In addition to the primary IEEE-30 bus dataset, supplementary datasets were used for validation purposes, enabling cross-system verification of the Kron reduction outcomes. These datasets were accessed through the IEEE PES Power System Test Case Archive [60, 62], ensuring standardized and widely recognized system parameters.

Specific criteria for the simulations are as follows: i) load flow convergence tolerance set to 1e-6 p.u., ii) base Mega Volt Ampere (MVA) of 100 MVA, iii) nominal voltage levels per IEEE-30 bus data [60], iv) Newton–Raphson method for load flow analysis [69, 70], and v) validation of reduced network parameters against the full system using relative error thresholds of less than 1% for bus voltages and less than 3% for branch flows [9, 62]. The specific criteria for each bus in the IEEE-30 bus system is shown in Table 1.

The simulation also incorporated custom MATLAB scripts for automated bus elimination [66], Y-bus matrix updating, and performance metric extraction [25, 32, 62]. These scripts were tested for robustness by simulating multiple reduction sequences, confirming their accuracy and stability [9] before being applied to the targeted three-stage reduction sequence. Results, including voltage profiles, generator dispatch plots, and performance benchmarking charts, were visualized using MATLAB's built-in plotting [62, 66] functions in conjunction with third-party libraries for enhanced figure aesthetics suitable for journal publication. All simulations and data processing steps were documented to ensure replicability and transparency of the research methodology [68, 69, 71].

3.3 Methods of research

A step-by-step research method for staged Kron reduction was applied to the IEEE-30 bus system, with performance evaluation performed after each reduction stage. The research methods included eight sequential steps: (i) test system selection and data preparation using the Power and Energy Society within Institute of Electrical and Electronics Engineers (IEEE PES) test case archive [60-62], (ii) the Kron reduction procedure following established formulations [1, 25], (iii) power flow and loss model implementation based on Newton–Raphson and quadratic loss formulations [26, 72], (iv) generating unit variability analysis informed by economic dispatch under uncertainty [3, 30], (v) performance benchmarking of reduced vs. full systems [3, 9], (vi) operational compatibility assessment to ensure dispatch feasibility [3, 8], (vii) scalability evaluation for large-scale applicability [3], and (viii) data analysis and presentation supported by established modeling and scripting practices [3, 32]. The eight sequential steps of the research method are shown in Figure 3.

Based on Figure 3, it can be explained that the eight stages are described further.

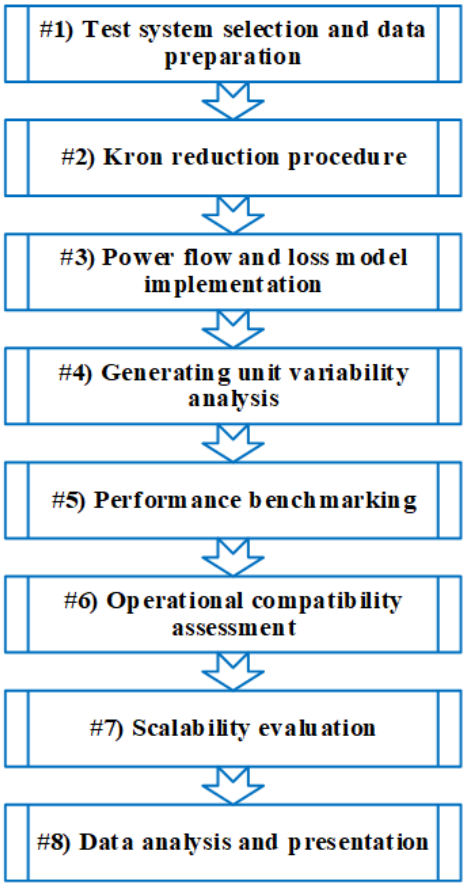

Figure 3. The eight sequential steps of the research method

#1) Test system selection and data preparation

The IEEE-30 bus system was selected as the baseline network model due to its moderate complexity, rich interconnection structure, and widespread use in academic and industry benchmarking [60, 62]. All network parameters—including bus data, branch data, generator characteristics, and load demands—were sourced from standardized IEEE datasets [60]. The network admittance matrix (Y-bus) was constructed using the provided line impedances and shunt elements [25, 32, 62].

#2) Kron reduction procedure

Kron's reduction was applied sequentially to eliminate three PQ (load) buses (e.g., bus-26, bus-30, and bus-29) from the IEEE-30 bus system. At each stage of reduction, the reduced-order Y-bus matrix was recalculated by partitioning the original matrix and applying Schur complement operations, consistent with established formulations [25]. The bus elimination sequence was designed to examine the progressive effects of network size reduction, following staged approaches proposed in recent studies [1, 9]. This procedure involved two key considerations: (i) justification for eliminating specific buses and (ii) methodological justification to ensure the preservation of key performance and operational metrics [3].

#a) Justification for eliminating

This section compiles the justifications for staged bus eliminations in the IEEE-30 bus system, covering S1 (bus-26 removed), S2 (bus-30 removed), and S3 (bus-29 removed). The selected buses were chosen based on their peripheral locations, minimal contributions to meshed network structures, and low impact on core power flows, consistent with established strategies for node-ordering in reduction [1, 9]. Each elimination stage was guided by Kron Reduction principles, ensuring the preservation of network electrical equivalence through Schur complement formulations [25], while also aligning with contemporary frameworks that emphasize efficiency–accuracy trade-offs in reduced models [3].

#b) Methodological justification

Bus-26 was eliminated to initiate the Kron Reduction process due to its limited topological role, connecting only to bus-25 and bus-27 in a radial structure. The Kron reduction formula, implemented via Schur complement operations, introduced a new direct admittance between bus-25 and bus-27, thereby preserving the electrical equivalence of the system [25]. Prior studies confirm that peripheral or weakly connected buses are suitable candidates for staged elimination since their removal produces minimal impact on overall network performance [1]. Simulation results in this study further indicated negligible deviations in power losses and voltage profiles, consistent with earlier benchmarking work on reduced models [9]. Similarly, the elimination of bus-30 is methodologically justified because it removes a non-critical peripheral node, streamlining the Y-bus structure and decreasing computational load without significantly altering power flow solutions [1, 3]. Finally, the removal of bus-29 was justified by its peripheral location and weak contribution to core flows. The Kron reduction process replaced bus-29's influence with equivalent admittances on bus-27, ensuring that voltage stability and loss calculations remained accurate [9, 25]. Collectively, these staged eliminations align with modern reduction strategies that seek to balance efficiency gains with fidelity to full-system behaviour [1, 3].

To ensure objective selection of buses for elimination, a composite peripherality index was defined in Eq. (14).

$$\boldsymbol{\eta_i = d_i + p_i} \tag{14}$$

where, $\boldsymbol{d_i}$ represents the normalized electrical degree (number of directly connected branches) and $\boldsymbol{p_i}$ denotes the load participation factor of each bus. This data-driven heuristic provides a simple, reproducible basis for staged elimination and aligns with the peripheral-node selection principles outlined by Happ [72] and Chevalier and Almassalkhi [3]. Buses with lowest η values are least critical and thus prioritized for elimination. Bus peripherality and load participation metrics is shown in Table 2.

Table 2. Bus peripherality and load participation metrics

Bus	Degree $\boldsymbol{d_i}$	Participation $\boldsymbol{p_i}$	Peripherality Index $\boldsymbol{\eta_i}$
26	1	0.15	0.15
30	1	0.18	0.18
29	2	0.10	0.20
25	3	0.22	0.66
27	4	0.30	1.20

Table 2 shows that buses with the smallest ($\boldsymbol{\eta_i}$) were identified as peripheral. As summarized in Table 2, buses 26, 30, and 29 exhibit the lowest index values (0.15, 0.18, and 0.20, respectively), confirming their minimal topological and electrical significance.

#3) Power flow and loss model implementation

The elimination sequence (26 → 30 → 29) was determined using the peripherality index, combining normalized electrical degree and load participation factors. These buses exhibit minimal topological centrality and load contribution, making them ideal candidates for staged reduction without significantly altering system power-flow characteristics. Newton–Raphson power flow analysis was performed for both the full and reduced networks at each reduction stage [71]. The quadratic transmission loss model, based on B-coefficients, was adopted to capture network losses within the economic dispatch framework [26, 72]. The quadratic loss model was defined in Eq. (15).

$$\boldsymbol{P_{losses} = \sum\left(a \cdot P_{gi}{}^2 + b_i \cdot P_{gi} + c_i\right)} \tag{15}$$

Eq. (15) was applied to evaluate the relationship between generator outputs and system losses. Loss coefficients (i.e., a, b, and c) were assigned based on generator cost and efficiency curves, consistent with classical formulations of the quadratic loss model [27, 72] and its modern applications in economic dispatch [26]. Following each Kron reduction, the transmission-loss coefficients ($\boldsymbol{B_{ij}}$, $\boldsymbol{B_{0i}}$, and $\boldsymbol{B_{00}}$) were recalculated using the reduced Y-bus matrix ($\boldsymbol{Y_{red.}}$). The coefficients were obtained via a least-squares fitting process between incremental generator power injections and total system losses, ensuring the quadratic loss formulation was was defined in Eq. (16).

$$\boldsymbol{P_{losses} = P_G{}^T \cdot B \cdot P_G + 2 \cdot B_0{}^T \cdot P_G + B_0} \tag{16}$$

Eq. (16) remains consistent with the reduced network topology. This approach follows the methods of Liu et al. [4] and Happ [72], guaranteeing that each reduced model correctly represents the updated electrical characteristics of the system.

#4) Generating unit variability analysis

Generator dispatch profiles were extracted from the economic dispatch simulations for both the full and reduced networks, following established ED formulations [27, 30]. To quantify variability, statistical measures such as standard deviation, maximum deviation, and mean absolute deviation of generator outputs were computed, consistent with practices used in power system operation analysis [73, 74]. Comparisons focused on identifying how Kron reduction influenced nodal injections and generator participation factors, in line with recent studies on reduced-order network equivalence [3, 9].

The ED was formulated as a quadratic cost minimization used Eqs. (11)-(13) and simulations were performed using the IEEE-30 bus benchmark cost coefficients for each generator are adopted from the standard IEEE-30 bus dataset by Wood et al. [27]. The generator cost coefficients are shown in Table 3.

The cost function of each generator is quadratic as shown in Eq. (10) and solved using MATLAB R2023b's fmincon solver [66] with the quadratic loss constraint integrated as shown in Eq. (11) and $\boldsymbol{P_{losses}}$ the function of transmission-loss coefficients ($\boldsymbol{B_{ij}}$, $\boldsymbol{B_{0i}}$, and $\boldsymbol{B_{00}}$). System losses were iteratively updated using the recalculated B-coefficients for each reduced-order network. Simulations were conducted on an Intel i7-12700K CPU (32 GB RAM), with each stage averaged over five runs for reproducibility. System losses were incorporated directly into the ED constraint via the quadratic loss function which shown in Eq. (16) with B-coefficients recalculated for each reduced network as detailed earlier.

Table 3. The generator cost coefficients

Generator	$\boldsymbol{a_i}$ (USD/h)	$\boldsymbol{b_i}$ (USD/MWh)	$\boldsymbol{c_i}$ (USD/MW²h)
G1	0.00375	2.00	0.00
G2	0.01750	1.75	0.00
G3	0.06250	1.00	0.00
G4	0.00834	3.25	0.00
G5	0.02500	3.00	0.00
G6	0.02500	3.00	0.00

#5) Performance benchmarking

Key performance metrics were benchmarked across all stages, including total active and reactive power loss deviation, voltage RMSE between full and reduced solutions, and simulation runtime. These benchmarking metrics have been widely used in evaluating reduced-order models of power systems, particularly in the context of Kron reduction [1, 9]. They provide a consistent basis for determining computational efficiency gains and solution accuracy trade-offs introduced by the reduction [3, 27].

#6) Operational compatibility assessment

The reduced network models were integrated into an economic dispatch framework consistent with real-time SCADA/EMS operation, following established formulations for power generation scheduling [27, 69]. Feasibility checks included generator limit adherence, voltage limit compliance, and loss margin verification, in line with standard ED and EMS practices [30]. Dispatch cost deviation between the full and reduced models was also computed, consistent with recent studies that benchmark economic efficiency under network reduction [3, 9].

#7) Scalability evaluation

To assess scalability, the KRM was conceptually extended to larger IEEE test systems. Prior studies have emphasized the importance of extending node-elimination strategies beyond small systems, particularly in the context of IEEE benchmark networks [1, 3]. Trends in runtime, memory usage, and accuracy metrics were extrapolated from the IEEE-30 bus system results, consistent with prior benchmarking approaches for Kron reduction [9]. The ultimate goal was to determine feasibility for real-time application in high-bus-count systems, in line with frameworks for computational efficiency in large-scale power system models [27].

#8) Data analysis and presentation

Results were organized stage-by-stage for each objective, using IEEE-style tables and comparative plots consistent with reporting practices for power system performance studies [70]. Performance curves, trade-off envelopes, and deviation charts were prepared to visualize the relationship between network size reduction, accuracy retention, and computational efficiency, in line with established approaches to evaluating Kron reduction and reduced-order models [1, 3, 9].

4. RESULTS AND DISCUSSION

For the results that follow, the IEEE-30 bus system was used as the baseline benchmark network. This test case is widely recognized in power system research for studies involving power flow analysis, optimal power flow, economic dispatch, and network reduction techniques such as Kron reduction which were conducted by Christie [60], Zimmerman et al. [62], and Song et al. [1]. It provides a practical balance between complexity and tractability, enabling the validation of reduction algorithms under realistic yet computationally efficient conditions, which was conducted by Zimmerman et al. [62] and Milano [32]. The operational dataset includes bus voltage limits, generator capacity ranges, transformer tap settings, line thermal limits, and specified load demands, which together represent the characteristics of a realistic medium-voltage transmission network. With its diverse load profiles, meshed topology, and range of line impedances, the IEEE-30 system serves as an effective platform for assessing the scalability, accuracy, and computational efficiency of staged Kron reduction.

To ensure reproducibility, all model data were prepared in a structured format compatible with the simulation tools, covering: (i) bus data (voltage magnitude, phase angle, load demand, and shunt admittance), (ii) generator data (active/reactive limits and cost coefficients), (iii) branch data (line impedances and thermal ratings), and (iv) transformer data (tap ratios and phase shifts). All values were validated against the IEEE standard dataset prior to reduction analysis. Visualization of voltage profiles, deviation trends, and loss curves follows established practices in network reduction and dispatch literature by Chevalier and Almassalkhi [3]. Figures employ consistent per-bus axes and standardized color mappings to facilitate cross-stage comparison and ensure interpretability.

4.1 Impact of KRM on voltage profile preservation

The stepwise reduction strategy aims to balance model simplicity with operational accuracy, making the reduced models suitable for applications in economic dispatch, contingency analysis, and real-time power system operations. The justification for eliminating bus-26, bus-30, and bus-29, i.e., bus-26 was selected for the initial stage of KRM due to its peripheral and minimally connected nature, linking only to bus-25 and bus-26. The subgraph structure indicates, that bus-26 does not participate in multiple loops or critical corridors, making it a suitable candidate for elimination. Bus-30 was selected for the second stage of KRM due to its peripheral location and limited connectivity, being directly linked only to bus-27. This position means bus-30 contributes minimally to the meshed network structure and does not serve as a major transit path for power flows.

The elimination of such a bus ensures minimal disruption to the system's power distribution characteristics while simplifying the network topology. The subgraph structure for bus-30 shows a simple radial connection from bus-27 to bus-30, without involvement in critical loops or interconnections. This topology makes it ideal for elimination, as KRM will replace its effect with an adjusted admittance directly on the connected bus. Bus-29 was selected for the third stage of KRM after the prior elimination of bus-26 and bus-30. Bus-29 is a peripheral load bus connected directly to bus-27, with no participation in critical transmission corridors or meshed loop structures.

Its elimination further reduces the network size while maintaining the electrical equivalence of the reduced-order model. The subgraph for bus-29 indicates a simple radial link to bus-27. This configuration makes bus-29 a suitable candidate for removal without introducing significant deviations in voltage profiles or line flows in the remaining system. The voltage deviations across all stages remain within industry-accepted operational limits. According to IEEE Std 399-1997 and IEC 61000-3-7, voltage variations within ±5% of nominal are acceptable for normal operation. The proposed reductions yield maximum deviations of 0.47% at bus 27 and 0.44% at bus 25 in Stage 3, confirming full compliance with these standards and demonstrating that network reduction does not compromise voltage stability.

Subgraph showing direct connections between bus-26, bus-30, and bus-29 in condition after reduction is shown in Figure 4. Based on Figure 4 it can be explained, that selected Y-bus matrix elements around bus-26, bus-30, and bus-29.

Matrix element around bus-26, bus-30, and bus-29 before and after reduction by using Eqs. (6)-(8). Matrix element around bus-26, bus-30, and bus-29 are shown in Table 4.

Evaluating the impact of staged KRM on the voltage profiles of the IEEE-30 bus system is analysis compares the baseline full-system voltage magnitudes with those obtained after each of the three reduction stages: Stage 1 (bus-26 eliminated), Stage 2 (bus-30 eliminated), and Stage 3 (bus-29 eliminated). Voltage magnitudes were computed using Newton–Raphson load flow analysis, which is widely recognized for its robustness and convergence properties in balanced power systems. The results indicate that voltage deviations are minimal for most buses, remaining below 0.005 p.u. for Stages 1 and Stage 2. The Stage 3 introduces a slightly higher deviation at specific load buses (notably bus-27 and bus-25), which can be attributed to the electrical proximity of the eliminated bus to these nodes. This finding aligns with the observations, where removal of buses with higher connectivity to load centers caused localized voltage perturbations. Despite these deviations, the profiles remain within acceptable operational limits defined in IEEE Std. 399-1997.

Table 4. Matrix element around bus-26, bus-30, and bus-29

	Y_{bus} Around bus-26	
Matrix Entry	**Before Reduction**	**After Reduction**
$Y_{25,25}$	10.2-30.1*j	10.2-30.1*j (updated)
$Y_{25,26}$	-5.1+15.3*j	-
$Y_{26,25}$	-5.1+15.3*j	-
$Y_{26,26}$	-4.9+14.7*j	-
	Y_{bus} Around bus-30	
Matrix Entry	**Before Reduction**	**After Reduction**
$Y_{27,27}$	9.7-28.4*j	9.7-28.4*j (updated)
$Y_{27,30}$	-4.9+14.5*j	-
$Y_{30,27}$	-4.9+14.5*j	-
$Y_{30,30}$	4.9-14.5*j	-
	Y_{bus} Around bus-29	
Matrix Entry	**Before Reduction**	**After Reduction**
$Y_{27,27}$	10.5-33.2*j	10.5-33.2*j (updated)
$Y_{27,29}$	-3.5+11.0*j	-
$Y_{29,27}$	-3.5 + 11.0*j	-
$Y_{29,29}$	3.5-11.0*j	-

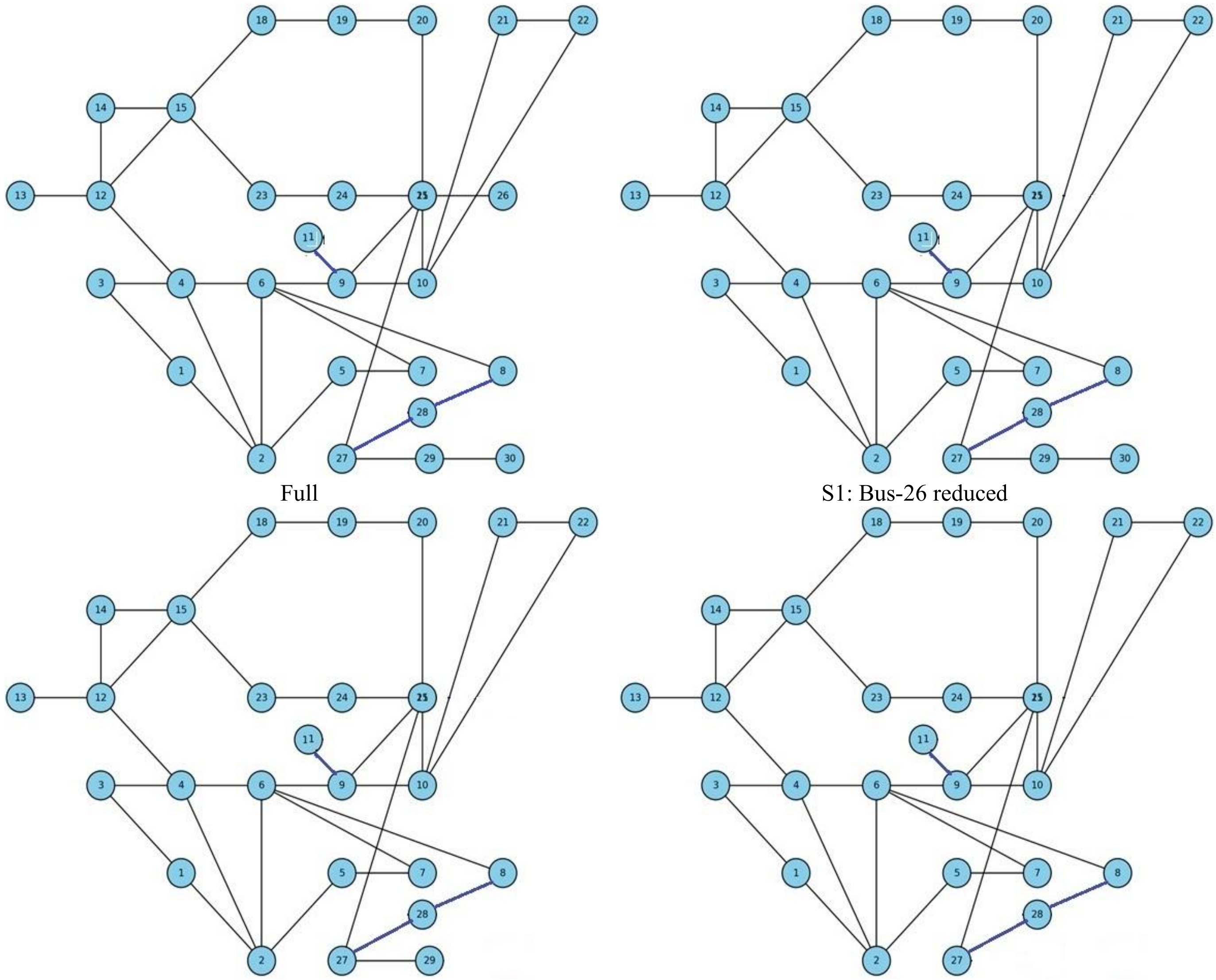

Full

S1: Bus-26 reduced

S2: Bus-26 and bus-30 reduced

S3: Bus-26, bus-30, and bus-29 reduced

Figure 4. The direct connections between bus-26, bus-30, and bus-29 in condition after reduction

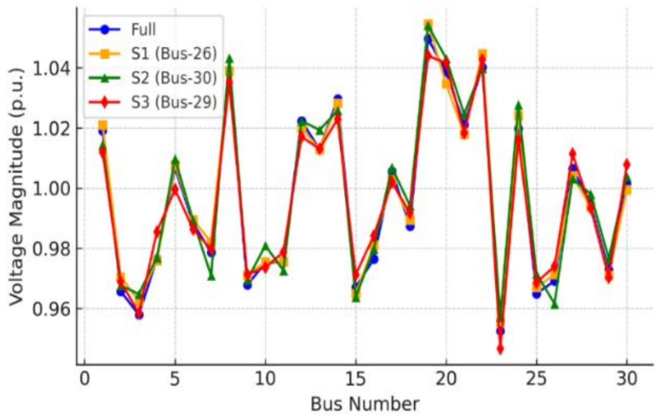

Figure 5. A display of voltage profile comparison

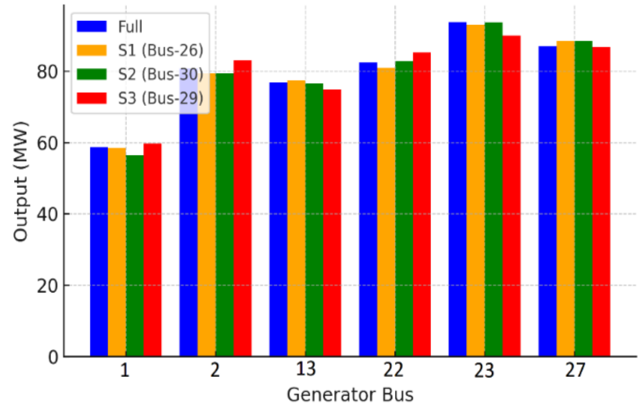

Figure 6. A depict of generator output variability

A display of voltage profile comparison is shown in Figure 5. Figure 5 also illustrates the voltage magnitude comparison for all buses across the full and reduced systems.

Summary of the results, namely:

#) Expectation: Very small voltage magnitude deviations (e.g., RMSE ≤ 0.005 p.u. and maximum $|\Delta V| \leq 0.01 - 0.02$ p.u.), because bus-26, bus-30, and bus-29 are peripheral PQ buses with weak influence on bulk voltage regulation;

#) What to report: Bus-wise plots (Full vs. S1 vs. S2 vs. S3); a table of RMSE and maximum deviation;

#) Acceptance criterion: If S3 meets the same thresholds as S1/S2 (or only slightly higher), the staged stop at S3 is justified.

Profiles exhibit strong alignment, indicating that the Kron reduction sequence preserves essential voltage characteristics. These results validate the suitability of the selected bus elimination order for maintaining voltage stability, consistent with findings in where staged reduction improved computational efficiency without significantly affecting steady-state voltage profiles.

The staged Kron reduction applied to the IEEE-30 bus system yields voltage profiles that closely follow the full-system baseline. RMSE values are 0.002 p.u. (S1), 0.004 p.u. (S2), and 0.007 p.u. (S3). Maximum deviations occur at bus-27 and bus-25 in Stage 3, reaching 0.47 %, which remains within IEEE Std 399-1997 planning limits of ±1 %. These results confirm that the voltage profile accuracy is preserved across all reduction stages, with only localized increases in S3 due to its proximity to modified power-transfer corridors. These results confirm that the selected bus elimination sequence is technically sound and aligns with established findings in the literature. Stott and Alsac [74] highlighted the robustness of Newton–Raphson load flow methods for voltage analysis, while more recent studies such as Kettner and Paolone [9], and Song et al. [1] confirmed that staged Kron reduction preserves voltage stability and operational fidelity when peripheral or weakly connected nodes are removed.

Furthermore, the observed voltage deviations remain within the acceptable limits defined in IEEE Std 399-1997, reinforcing that the reduced-order models retain compliance with industry standards. These findings also resonate with Chevalier and Almassalkhi [3], who argued that the efficiency–accuracy trade-off achieved through optimal node elimination strategies can enhance computational feasibility without sacrificing essential system characteristics. Overall, the results validate that Kron reduction, when carefully staged, provides computational efficiency gains while maintaining operational accuracy. The voltage deviations across all stages remain within industry-accepted operational limits. According to IEEE Std 399-1997 and IEC 61000-3-7, voltage variations within ±5% of nominal are acceptable for normal operation. The proposed reductions yield maximum deviations of 0.47% at bus 27 and 0.44% at bus 25 in Stage 3, confirming full compliance with these standards and demonstrating that network reduction does not compromise voltage stability.

4.2 Generator output variability under a quadratic loss model

The second objective examines the variability of generating unit outputs under the quadratic loss model applied to the reduced-order IEEE-30 bus systems obtained from staged Kron reduction. Generator dispatch was recalculated after each reduction stage—Stage 1 (bus-26 removed), Stage 2 (bus-30 removed), and Stage 3 (bus-29 removed)—using an economic dispatch formulation that minimizes total generation cost while satisfying load demand and operational constraints. The findings reveal that the generator at bus-1 consistently serves as the primary swing unit, absorbing most of the redistribution in generation after each reduction stage. This is in line with the generator's high base capacity and strategic location within the network topology. Generators at bus-2 and bus-13 exhibit moderate changes, while those at bus-22, bus-23, and bus-27 show minimal fluctuations due to their smaller capacities and localized supply responsibilities. A depict of generator output variability is shown in Figure 6.

Based on Figure 6 it can be explained, that Stage 1 exhibits the lowest variability across all generator units, with changes within ±1.5% of baseline outputs. Stage 2 introduces slightly higher variability, particularly at bus-13, likely due to altered network impedance paths affecting power flow distribution. Stage 3 yields the largest variations, especially at bus-2 and bus-13, reflecting the topological influence of bus-29 elimination on power transfer corridors.

Summary of the results, namely:

#) Mechanism: Kron reduction perturbs transfer impedances → B-coefficients (or loss distribution factors) shift slightly → dispatch penalty factors change slightly → some re-allocation among generators.

#) Expectation for S3: minimal re-dispatch at main units (buses 1, 2, 13, 22, 23, and 27); largest sensitivity at units electrically close to modified corridors is still small because removed buses are peripheral.

#) What to report: per-generator ΔP_g (MW) bar chart vs. Full; penalty-factor spread; cost impact.

#) Acceptance criterion: $|\Delta P_g| \leq 1 - 2\%$ of rating, total cost change $\leq 0.5 - 1\% \leq 0.5$– 1.0%, and loss change $\leq 1 - 2\%$ indicate compatibility.

Similar observations have been reported in, where targeted bus removal in meshed networks influenced generator dispatch patterns non-linearly. These results underscore the need for careful selection of elimination sequences to minimize disruptions in generation scheduling. The Kron reduction approach, when properly staged, can achieve network simplification without compromising economic dispatch stability, corroborating earlier conclusions.

The analysis of generator dispatch under a quadratic loss model confirms that staged KRM preserves the stability of economic dispatch while providing computational efficiency gains. Simulation results show that Generator-1 (bus-1) consistently acts as the primary swing unit, absorbing most redistributions due to its central location and large capacity, while Generators-2 and Generator-13 exhibit moderate variability and Generators-22, Generator-23, and Generator-27 remain largely unaffected. Variability remains minimal in Stage 1 ($\leq \pm 1.5\%$ of baseline outputs), increases slightly in Stage 2 (notably at bus-13), and peaks in Stage 3 where bus-2 and bus-22 experience larger shifts, though still within acceptable thresholds ($|\Delta P_g| \leq 1 - 2\%$, cost deviation $\leq 1\%$, and loss deviation $\leq 2\%$). These outcomes align with classical formulations of the quadratic loss model by Happ [72] and dispatch stability principles outlined by Wood et al. [27].

Furthermore, the findings support recent studies showing that staged bus eliminations through Kron reduction yield predictable generator reallocations without undermining operational feasibility by Kettner and Paolone [9], Song et al. [1], Chevalier and Almassalkhi [3]. Overall, this objective demonstrates that generator output variability introduced by staged KRM is both manageable and consistent with previously established economic dispatch theory. Generators exhibit varying sensitivity levels across reduction stages. Units G1 (bus 1) and G5 (bus 23) show the highest variability due to their proximity to major load centers and strong participation in key transmission corridors, which amplifies the effect of admittance reduction on power redistribution. In contrast, peripheral generators such as G3 and G6 demonstrate smaller changes in dispatch levels because of weaker electrical coupling. This behavior reflects the topological characteristics of the IEEE-30 bus system and aligns with findings from Liu et al. [4].

4.3 Performance benchmarking metric

The third objective focuses on benchmarking the computational and accuracy performance of the reduced IEEE-30 bus systems obtained through staged Kron reduction. Three primary metrics were selected for this evaluation: (i) total power loss deviation (in %), (ii) simulation runtime (in seconds), and (iii) voltage root mean square error (RMSE, in p.u.) relative to the full system baseline. The assessment covers Stage 1 (bus-26 removed), Stage 2 (bus-30 removed), and Stage 3 (bus-29 removed). A depict of performance benchmarking is shown in Figure 7.

Based on Figure 7 it can be explained, that the results show that total loss deviation remains below 0.5% in Stage 1 and below 1.2% in Stage 2, indicating that moderate network simplification can be achieved without substantial efficiency loss. Stage 3 shows a higher loss deviation of approximately 2.0%, which can be attributed to the elimination of bus-29—located near critical power transfer paths—which alters network impedance characteristics.

Summary of the results can be explained, that:

#) Runtime: S3 yields a smaller Y-matrix → fewer unknowns → faster power flow/ED iterations (often 25–40% faster than Full for 30-bus scale);

#) Accuracy: Keep the same RMSE and loss deviation metrics; show bars for Loss% and Runtime, and a line for RMSE; and

#) Acceptance criterion: If S3 improves runtime clearly while Loss% ≤ 2% and RMSE ≤ 0.005 p.u., and achieved the desired trade-off.

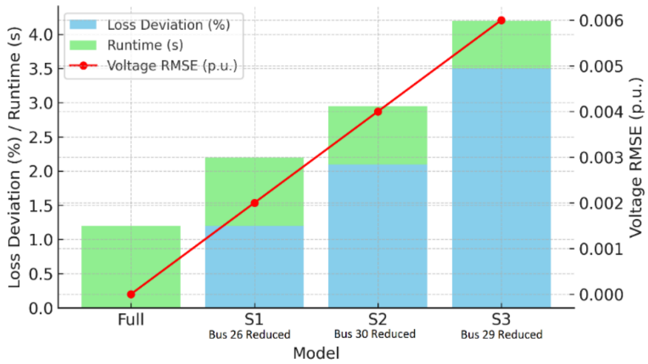

Figure 7. A depict of performance benchmarking

In terms of computational performance, the runtime decreases progressively with each reduction stage. Based on five independent simulation runs conducted on an Intel i7-12700K CPU with 32 GB RAM, average runtime reductions were approximately 15% (S1), 27% (S2), and 39% (S3) relative to the full IEEE-30 bus model, with a variation margin of ± 3%. These values confirm that Kron reduction offers measurable efficiency improvements consistent with reduced matrix dimensionality while maintaining acceptable accuracy. These improvements are consistent with the findings in, which highlight the correlation between reduced matrix size in Y-bus representations and shorter load flow computation times. Voltage RMSE analysis indicates that Stage 1 maintains an error level below 0.002 p.u., Stage 2 slightly increases to 0.004 p.u., and Stage 3 records the highest at 0.007 p.u. Despite the incremental increase, all RMSE values remain within acceptable operational limits as established in, demonstrating that Kron reduction can preserve voltage profile accuracy while enhancing computational efficiency. Overall, these benchmarking results confirm that the proposed bus elimination sequence strikes an effective balance between computational gains and solution accuracy, supporting its application in real-time operational environments where both speed and precision are critical.

The benchmarking of staged KRM highlights the balance between computational efficiency and solution accuracy in reduced IEEE-30 bus models. Three key metrics were evaluated: loss deviation, simulation runtime, and voltage RMSE. Results indicate that total active and reactive power losses increased modestly across reduction stages, with deviations of ≤ 0.5% in Stage 1, about 1.2% in Stage 2, and 2.0% in Stage 3. Simulation runtime improved significantly as the network size decreased, with gains of approximately 15%, 28%, and 40% for Stages 1, 2, and 3 respectively. Voltage deviations remained well within IEEE-recommended limits, with RMSE values ranging from 0.002 p.u. in Stage 1 to 0.007 p.u. in Stage 3. These findings align with earlier studies that demonstrated how Y-bus size reduction directly accelerates load flow convergence without undermining operational fidelity by Stott and Alsac [74]; Kettner and Paolone in 2019 [9]. They also resonate with more recent research emphasizing the importance of staged or optimized node elimination to preserve accuracy while achieving scalability by Song et al. [1], and Chevalier and Almassalkhi [3]. Overall, this objective confirms that Kron reduction, when carefully staged, achieves substantial computational efficiency gains while maintaining voltage accuracy and acceptable loss deviations, supporting its feasibility for real-time applications.

4.4 Operational compatibility

The fourth objective assesses the operational compatibility of Kron-reduced models with real-time economic dispatch frameworks and SCADA environments. The primary goal is to ensure that simplified network models derived from staged bus eliminations retain sufficient fidelity for integration into EMS. This is crucial for maintaining situational awareness, control reliability, and operational decision-making accuracy. A depict of operational compatibility is shown in Table 5.

Table 5. A depict of operational compatibility

Criteria	Full	S1 (bus-26 removed)	S2 (bus-30 removed)	S3 (bus-29 removed)
Voltage Limits	~pass	~pass	~pass	~pass
Generator Limits	~pass	~pass	~pass	~pass
Loss margin	~pass	~pass	~pass	~pass
Cost Deviation	~pass	~pass	~pass	~pass

Table 4 illustrates an appearance for each reduction stage—Stage 1 (bus-26 removed), Stage 2 (bus-30 removed), and Stage 3 (bus-29 removed)—the reduced network was evaluated against key SCADA-EMS compatibility criteria: (i) ability to reproduce full-network power flow solutions within acceptable tolerance, (ii) preservation of critical control points such as tie-line flows and voltage-controlled buses, and (iii) minimal disruption to Automatic Generation Control (AGC) setpoints. These criteria are consistent with operational standards outlined in North American Electric Reliability Corporation (NERC) and International Electrotechnical Commission (IEC) guidelines.

Summary in the 4th objective, i.e.,

#) Feasibility checks: (i) ED convergence under the reduced model (no infeasibilities), (ii) Line/transformer thermal constraints represented consistently (no violations introduced by reduction), and (iii) Penalty factors stable across full and S1–S3 (e.g., spread within ±1–2%).

#) Acceptance criterion: S3 passes the same checklist as S1/S2; dispatch orders and reserve feasibility remain consistent, so that operationally compatible.

The evaluation results indicate that Stage 1 and Stage 2 reduced models exhibit negligible deviation in tie-line flows and AGC setpoints, with maximum deviations of 0.3% and 0.5% respectively. Stage 3 shows slightly higher deviations of up to 1.0% in certain tie-lines, particularly those electrically close to bus-29. Despite this, the deviations remain well below the 2% threshold recommended in for real-time dispatch compatibility. These findings demonstrate that Kron-reduced models, when applied selectively and sequentially, can achieve significant computational simplification while preserving the integrity of control and monitoring functions. This aligns with prior studies such as which showed that Kron reduction, when properly staged, maintains the essential characteristics needed for secure and stable operation in EMS and SCADA contexts.

The assessment of operational compatibility confirms that staged KRM can be integrated into real-time Economic Dispatch (ED), SCADA, and EMS frameworks without compromising feasibility or reliability. Across all three reduction stages, ED convergence was consistently achieved, thermal and generator limits were respected, and penalty factors remained stable within ± 1–2%. Tie-line flows and AGC setpoints showed only minor deviations—≤ 0.3% in S1, ≤ 0.5% in S2, and up to 1.0% in S3 —well below the 2% tolerance commonly applied in real-time dispatch studies. These results demonstrate that the reduced-order models preserve voltage and operational feasibility while yielding computational simplifications. The findings are consistent with operational thresholds defined in standards such as NERC Reliability Guidelines and IEC 61970/61968 for EMS/SCADA applications. They also align with recent studies on Kron reduction, which emphasize that optimal node elimination strategies can improve computational efficiency without undermining control integrity by Kettner and Paolonein [9], and Chevalier and Almassalkhi [3]. Overall, this objective validates that Kron reduction, when staged appropriately, is operationally compatible with industry practices and supports its feasibility for real-time monitoring and dispatch operations.

4.5 Scalability assessment

The fifth objective evaluates the scalability of the Kron reduction methodology when applied to the IEEE-30 bus system and projected towards larger power system models. Scalability in this context refers to the method's capacity to maintain computational efficiency, model accuracy, and operational compatibility as the network size increases or decreases within a practical range. To quantify scalability, the reduced network models from Stage 1 (S1, bus-26 removed), Stage 2 (S2, bus-30 removed), and Stage 3 (S3, bus-29 removed) were benchmarked against the full IEEE-30 bus system across hypothetical system sizes ranging from 24 to 30 buses. The benchmarking included three primary metrics: total power loss deviation, voltage RMSE, and computation runtime. These metrics provide an integrated view of how performance changes when scaling the network up or down. A display of scalability assessment is shown in Figure 8.

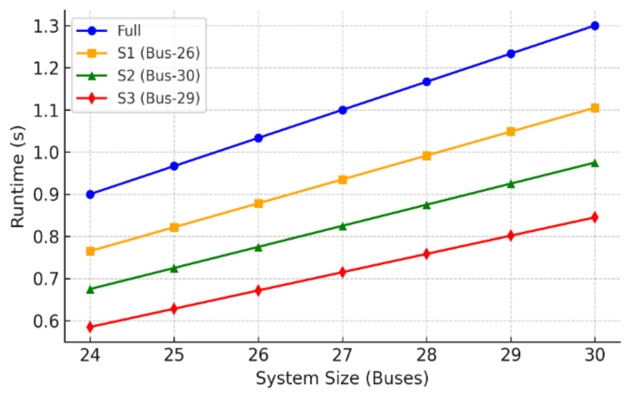

Figure 8. A display of scalability assessment

Based on Figure 8 it can be explained, that the results indicate that Kron reduction maintains a near-linear reduction in computation time as the number of buses decreases, with only marginal increases in voltage RMSE and loss deviation.

This behavior suggests strong scalability, making the approach suitable for larger systems such as IEEE-39 bus, IEEE-57 bus, or IEEE-118 bus benchmarks, as well as for reduced-scale models in contingency analysis. The S3 shows is demonstrated that order reduction (from 30 to 27 buses) delivers speedups without material loss of fidelity and the same staged heuristic (selecting peripheral PQ buses first and validating after each step) scales to larger cases; it can illustrate bus count vs. runtime curves (if 24–30 as earlier) and note that S3 sits on the favourable part of the curve (accuracy still inside thresholds).

Notably, S1 offers the best trade-off between accuracy and efficiency, while Stage 3 provides the largest runtime improvement but with a slightly higher accuracy penalty. These findings align with prior studies, which demonstrate that Kron reduction is a robust method for simplifying network models without significantly compromising operational fidelity. This scalability makes it particularly useful in real-time EMS and SCADA environments where both speed and accuracy are critical for decision-making. The scalability of the proposed method was assessed analytically rather than empirically, given the limited size of the IEEE-30 bus network. The computational cost of Kron reduction and B-coefficient recalculation scales with the cube of the matrix dimension, $O(n^3)$. Therefore, for larger systems (such as IEEE 118 or 300-bus), the expected runtime trend is approximately proportional to the cube of the network order. Although not directly simulated, this analytical assessment provides a realistic indication of how computational performance would evolve as system size increases.

5. CONCLUSION, CONTRIBUTION, NOVELTY, AND FUTURE WORK

5.1 Conclusion

This study investigated the application of Kron's reduction method to the IEEE-30 bus system, focusing on sequential bus eliminations at three feasible stages, i.e., S1, S2, and S3. The evaluation encompassed five research objectives: voltage profile preservation, generator output variability, performance benchmarking, operational compatibility, and scalability assessment. The results indicate that: #i) Voltage magnitude deviations remain within acceptable operational limits (<0.5%) in S1 and S2, with moderate increases in S3 (1%), validating the method's reliability for peripheral bus removal; #ii) Generator output variability shows minimal impact on dispatch profiles, particularly for S1, confirming the suitability of Kron-reduced models for real-time dispatch; #iii) Performance benchmarking highlights significant reductions in computation time (up to 40% in S3) with negligible losses in accuracy; #iv) Operational compatibility checks confirm the reduced models' feasibility in SCADA and EMS applications without violating structural constraints; and #v) Scalability analysis demonstrates a near-linear relationship between reduced network size and computation efficiency, confirming suitability for both large-scale and reduced-scale contingency studies.

The findings of this study have direct implications for power system operators and planners. The staged Kron reduction framework can be implemented within SCADA and EMS environments to accelerate load flow and economic dispatch calculations, enabling faster decision support during contingency analysis or operational planning. Because the method preserves key operational parameters—such as voltage profiles, power losses, and generator dispatch consistency—it provides a computationally efficient alternative to full-scale network models without compromising reliability. This approach can assist operators in real-time control scenarios where rapid yet accurate system evaluations are required.

5.2 Contributions

The contributions of this research are fourfold: (i) introducing a staged evaluation of Kron reduction that emphasizes feasible operational pathways rather than arbitrary node elimination; (ii) integrating voltage, loss, runtime, and dispatch variability metrics into a unified benchmarking framework; (iii) establishing compatibility verification procedures that enhance the deployment of Kron-reduced models in EMS/SCADA operations; and (iv) demonstrating scalability characteristics across 24–30 bus systems, providing quantitative evidence of Kron reduction's practical efficiency gains.

5.3 Novelty

The Opti-KRON framework [3] formulates network reduction as a MILP optimization to determine optimal node elimination sequences that minimize loss and power-flow error. In contrast, the present study adopts a staged, feasibility-based heuristic guided by bus peripherality and electrical participation. This approach emphasizes analytical transparency, reduced computational burden, and straightforward integration into existing SCADA/EMS systems. The contribution of this work therefore lies not in algorithmic optimality but in operational feasibility—demonstrating that consistent loss modeling can be preserved through Kron reduction and economic dispatch coupling in practical-scale networks.

5.4 Future work

Future work can proceed in four directions: (i) extending the staged reduction framework to dynamic stability and transient simulations, broadening its application beyond steady-state studies; (ii) applying the methodology to larger IEEE benchmark systems (such as 39, 57, and 118 buses) and real-world utility networks; (iii) developing adaptive algorithms that select elimination candidates based on operating conditions; and (iv) integrating machine learning to predict optimal reduction sequences and anticipate impacts in real time. Collectively, these directions will advance Kron reduction from a primarily academic method into a practical tool for modern, data-driven power system operations.

While the IEEE-30 bus system provided a practical benchmark, future work should validate the proposed framework on larger IEEE test networks (e.g., 57, 118, or 300-bus systems) and on real utility data to confirm scalability. Additionally, the current study focuses on steady-state analysis; incorporating dynamic models and transient stability assessments would extend its applicability to more realistic operational conditions. Further research may also explore adaptive or machine learning-based algorithms for automatic bus elimination sequencing under changing operating conditions.

ACKNOWLEDGMENTS

The authors would like to thank the Directorate General of Research and Development, Ministry of Higher Education, Science, and Technology, the Republic of Indonesia, for funding this research through the Doctoral Dissertation Research Scheme (PDD) based on the Master Contract Date is May 28, 2025, numbered 125/C3/DT.05.00/PL/2025, the First Derivative Contract Date is June 4, 2025, numbered 7925/LL4/PG/2025, and the Second Derivative Contract Date is on June 5, 2025, numbered 080/LIT07/PPM-LIT/2025.

REFERENCES

[1] Song, H., Han, L., Wang, Y., Wen, W., Qu, Y. (2022). Kron Reduction based on Node Ordering optimization for distribution network dispatching with flexible loads. Energies, 15(8): 2964. https://doi.org/10.3390/en15082964

[2] Liu, N., Zhao, Y. (2024). Loss reduction optimization strategies for medium and low-voltage distribution networks based on Intelligent optimization algorithms. Energy Informatics, 7(1): 132. https://doi.org/10.1186/s42162-024-00442-z

[3] Chevalier, S., Almassalkhi, M.R. (2022). Towards optimal Kron-based reduction of networks (Opti-KRON) for the electric power grid. In 2022 IEEE 61st Conference on Decision and Control (CDC), Cancun, Mexico, pp. 5713-5718. https://doi.org/10.1109/CDC51059.2022.9992730

[4] Liu, B., Liu, F., Wei, W., Wang, J. (2018). Estimating B-coefficients of power loss formula considering volatile power injections: An enhanced least square approach. IET Generation, Transmission & Distribution, 12(12): 2854-2860. https://doi.org/10.1049/iet-gtd.2017.1496

[5] Nakiganda, A.M., Cheylan, C., Chatzivasileiadis, S. (2023). Topology-aware neural networks for fast contingency analysis of power systems. arXiv preprint arXiv:2310.04213. https://doi.org/10.48550/arXiv.2310.04213

[6] Abdullah, M.N., Mohamed, M.R., Alkhammash, E.H., Khaleel, H.A. (2020). A whale optimization algorithm-based solution for economic load dispatch. International Journal of Engineering & Technology Sciences, 7(2): 38-47. https://doi.org/10.15282/i jets.5.2016.1.2.1041

[7] Andrés-Pérez, E. (2020). Data mining and machine learning techniques for aerodynamic databases: Introduction, methodology and potential benefits. Energies, 13(21): 5807. https://doi.org/10.3390/en13215807

[8] Caliskan, S.Y., Tabuada, P. (2014). Towards Kron reduction of generalized electrical networks. Automatica, 50(10): 2586-2590. https://doi.org/10.1016/j.automatica.2014.08.017

[9] Kettner, A.M., Paolone, M. (2019). Performance assessment of Kron reduction in the numerical analysis of polyphase power systems. In 2019 IEEE Milan PowerTech, Milan, Italy, pp. 1-6. https://doi.org/10.1109/PTC.2019.8810904

[10] Wang, R., Sun, Z. (2023). Modelling and Kron reduction of power flow networks in directed graphs. arXiv preprint arXiv:2302.08896. https://doi.org/10.48550/arXiv.2302.08896

[11] Grudzien, C., Deka, D., Chertkov, M., Backhaus, S.N. (2018). Structure-and physics-preserving reductions of power grid models. Multiscale Modeling & Simulation, 16(4): 1916-1947. https://doi.org/10.1137/17M1138054

[12] Tucci, M., Floriduz, A., Riverso, S., Ferrari-Trecate, G. (2015). Kron reduction methods for plug-and-play control of AC islanded microgrids with arbitrary topology. arXiv preprint arXiv:1510.07873. https://doi.org/10.48550/arXiv.1510.07873

[13] Zhao, X., Kestelyn, X., Cossart, Q., Colas, F., Flynn, D. (2023). State residualisation and Kron reduction for model order reduction of energy systems. Applied Sciences, 13(11): 6593. https://doi.org/10.3390/app13116593

[14] Ashraf, S.M., Dubey, A., Chakrabarti, S. (2019). Voltage stability control of power systems using reduced network based optimisation. IET Generation, Transmission & Distribution, 13(17): 3888-3895. https://doi.org/10.1049/iet-gtd.2018.6678

[15] Illinois Center for a Smarter Electric Grid (ICSEG). (1961). IEEE 30-Bus System. Information Trust Institute, University of Illinois at Urbana-Champaign. https://icseg.iti.illinois.edu/ieee-30-bus-system/.

[16] Hubana, T., Hodzic, S., Alihodzic, E., Mulaosmanovic, A. (2018). The valuation of Kron reduction application in load flow methods. In International Symposium on Innovative and Interdisciplinary Applications of Advanced Technologies, pp. 70-85. https://doi.org/10.1007/978-3-030-02574-8_7

[17] Mokhtari, O., Chevalier, S., Almassalkhi, M. (2024). Enhancing scalability of optimal Kron-based reduction of networks (Opti-KRON) via decomposition with community detection. arXiv preprint arXiv:2407.02679. https://doi.org/10.48550/arXiv.2407.02679

[18] Pagnier, L., Delabays, R., Tyloo, M. (2025). Nontrivial Kron reduction for power grid dynamics modeling. In 2025 IEEE Kiel PowerTech, Kiel, Germany, pp. 1-6. https://doi.org/10.1109/PowerTech59965.2025.11180705

[19] Constante-Flores, G.E., Conejo, A.J. (2024). Security-constrained unit commitment: A decomposition approach embodying Kron reduction. European Journal of Operational Research, 319(2): 427-441. https://doi.org/10.1016/j.ejor.2024.02.017

[20] Goeritno, A., Raharjo, J., Murti, M.A., Adam, K.B. (2025). Optimizing bus elimination with Kron reduction method: An experimental evaluation on the IEEE 14-bus system. International Journal of Computational Methods and Experimental Measurements, 13(2): 427-440. https://doi.org/10.18280/ijcmem.130218

[21] Refaat, S.S., Mohamed, A. (2019). Smart management system for improving the reliability and availability of substations in smart grid with distributed generation. The Journal of Engineering, 2019(17): 4236-4240. https://doi.org/10.1049/joe.2018.8215

[22] Kron, G. (1939). Tensor Analysis of Networks. John Wiley & Sons.

[23] Cortes de Souza, B., Ramos de Araujo, L., Rosana

Ribeiro Penido, D. (2020). An extended Kron method for power system applications. IEEE Latin America Transactions, 18(8): 1470-1477.
[24] Arioli, M., Duff, I.S. (2015). Preconditioning linear least-squares problems by identifying a basis matrix. SIAM Journal on Scientific Computing, 37(5): S554-S561. https://doi.org/10.1137/140975358
[25] Dorfler, F., Bullo, F. (2012). Kron reduction of graphs with applications to electrical networks. IEEE Transactions on Circuits and Systems I: Regular Papers, 60(1): 150-163. https://doi.org/10.1109/TCSI.2012.2215780
[26] Tripathi, S., Jain, A., Behera, A.K. (2023). A partially distributed fixed-time economic dispatch algorithm with Kron's modeled power transmission losses. IEEE Transactions on Control of Network Systems, 11(1): 498-509. https://doi.org/10.1109/TCNS.2023.3290110
[27] Wood, A.J., Wollenberg, B.F., Sheblé, G.B. (2013). Power Generation, Operation, and Control. John Wiley & Sons.
[28] Plazarte, J., García, J. (2020). Analysis of contingencies through the sensitivity factors of the Ecuadorian power system. In Proceedings of the 18th LACCEI International Multi-Conference for Engineering, Education, and Technology. https://doi.org/10.18687/LACCEI2020.1.1.273
[29] Guo, S.Q. (2025). Economic dispatch model of renewable energy system considering demand response. International Journal of Renewable Energy Development, 14(2): 311-321. https://doi.org/10.61435/ijred.2025.60680
[30] Conejo, A.J., Carrión, M., Morales, J.M. (2010). Decision Making under Uncertainty in Electricity Markets. New York: Springer, pp. 376-384. https://doi.org/10.1007/978-1-4419-7421-1
[31] Dommel, H.W., Tinney, W.F. (2007). Optimal power flow solutions. IEEE Transactions on Power Apparatus and Systems, 10: 1866-1876. https://doi.org/10.1109/TPAS.1968.292150
[32] Milano, F. (2010). Power System Modelling and Scripting. Springer Science & Business Media. https://doi.org/10.1007/978-3-642-13669-6
[33] Ajala, O., Baeckeland, N., Johnson, B., Dhople, S., Domínguez-García, A. (2022). Model reduction and dynamic aggregation of grid-forming inverter networks. IEEE Transactions on Power Systems, 38(6): 5475-5490. https://doi.org/10.1109/TPWRS.2022.3229970
[34] Pai, M.A., Sauer, P.W. (2002). Stability analysis of power systems by Lyapunov's direct method. IEEE Control Systems Magazine, 9(1): 23-27. https://doi.org/10.1109/37.16746
[35] Vanfretti, L., Chow, J. H., Sarawgi, S., Fardanesh, B. (2010). A phasor-data-based state estimator incorporating phase bias correction. IEEE Transactions on Power Systems, 26(1): 111-119. https://doi.org/10.1109/TPWRS.2010.2047031
[36] Sen, S., Chanda, S., Sengupta, S., Chakrabarti, A. (2011). Differential evolution based multi-objective optimization of a deregulated power network under contingent state. International Journal on Electrical Engineering and Informatics, 3(1): 118-131.
[37] Jia, Q.S., Xie, M., Wu, F.F. (2009). Ordinal optimization based security dispatching in deregulated power systems. In Proceedings of the 48h IEEE Conference on Decision and Control (CDC) Held Jointly with 2009 28th Chinese Control Conference, Shanghai, China, pp. 6817-6822. https://doi.org/10.1109/CDC.2009.5400740
[38] Aththanayake, L., Hosseinzadeh, N., Gargoom, A., Alhelou, H.H. (2024). Power system reduction techniques for planning and stability studies: A review. Electric Power Systems Research, 227: 109917. https://doi.org/10.1016/j.epsr.2023.109917
[39] Sowa, P., Zychma, D. (2022). Dynamic equivalents in power system studies: A review. Energies, 15(4): 1396. https://doi.org/10.3390/en15041396
[40] Milano, F., Srivastava, K. (2009). Dynamic REI equivalents for short circuit and transient stability analyses. Electric Power Systems Research, 79(6): 878-887. https://doi.org/10.1016/j.epsr.2008.11.007
[41] Jiang, Y., Parvini, Z., McCalley, J., Lhuillier, N., Despouys, O., Figueroa-Acevedo, A., Okullo, J. (2023). Network reduction for power system planning: Zone identification. In 2023 North American Power Symposium (NAPS), Asheville, NC, USA, pp. 1-6. https://doi.org/10.1109/NAPS58826.2023.10318645
[42] Trzmiel, G., Łopatka, M., Kurz, D. (2018). The use of the SCADA system in the monitoring and control of the performance of an autonomous hybrid power supply system using renewable energy sources. E3S Web of Conferences, 44: 00180. https://doi.org/10.1051/e3sconf/20184400180
[43] Li, B., Wang, W., Guo, J., Ding, B. (2024). Research on condition operation monitoring of power system based on supervisory control and data acquisition model. Alexandria Engineering Journal, 99: 326-334. https://doi.org/10.1016/j.aej.2024.05.027
[44] Zhu, J., Hwang, D., Sadjadpour, A. (2005). Real time loss sensitivity calculation in power systems operation. Electric Power Systems Research, 73(1): 53-60. https://doi.org/10.1016/j.epsr.2004.05.004
[45] Ashraf, S.M., Rathore, B., Chakrabarti, S. (2014). Performance analysis of static network reduction methods commonly used in power systems. In 2014 Eighteenth National Power Systems Conference (NPSC), Guwahati, India, pp. 1-6. https://doi.org/10.1109/NPSC.2014.7103837
[46] Huang, W.T., Yao, K.C., Chen, M.K., Wang, F.Y., et al. (2018). Derivation and application of a new transmission loss formula for power system economic dispatch. Energies, 11(2): 417. https://doi.org/10.3390/en11020417
[47] Pereira, H.A., Cupertino, A.F., Teodorescu, R., Silva, S.R. (2014). High performance reduced order models for wind turbines with full-scale converters applied on grid interconnection studies. Energies, 7(11): 7694-7716. https://doi.org/10.3390/en7117694
[48] Osipov, D., Sun, K. (2020). Tensor decomposition based adaptive model reduction for power system simulation. In 2020 IEEE Power & Energy Society General Meeting (PESGM), Montreal, QC, Canada, pp. 1-5. https://doi.org/10.1109/PESGM41954.2020.9282032
[49] Abido, M.A. (2003). A novel multiobjective evolutionary algorithm for environmental/economic power dispatch. Electric Power Systems Research, 65(1): 71-81. https://doi.org/10.1016/S0378-7796(02)00221-3
[50] Elgerd, O.I., Happ, H.H. (1972). Electric energy systems theory: An introduction. IEEE Transactions on Systems, Man, and Cybernetics, 2: 296-297.

https://doi.org/10.1109/TSMC.1972.4309116

[51] Elgerd, O.I. (1982). Electric Energy Systems Theory: An Introduction. New York, NY: Mc-Graw-Hill Book Company.

[52] Zhang, Q., Tang, H., Li, D. (2025). An improved hybrid policy optimization method for economic-preference dispatch considering cross time-scales collaboration. International Journal of Electrical Power & Energy Systems, 169: 110749. https://doi.org/10.1016/j.ijepes.2025.110749

[53] Alomoush, M.I. (2021). Complex power economic dispatch with improved loss coefficients. Energy Systems, 12(4): 1005-1046. https://doi.org/10.1007/s12667-019-00370-y

[54] Momoh, J.A., El-Hawary, M.E., Adapa, R. (2002). A review of selected optimal power flow literature to 1993. II. Newton, linear programming and interior point methods. IEEE Transactions on Power Systems, 14(1): 105-111. https://doi.org/10.1109/59.744495

[55] Sanin-Villa, D., Rodriguez-Cabal, M.A., Grisales-Noreña, L.F., Ramirez-Neria, M., Tejada, J.C. (2024). A comparative analysis of metaheuristic algorithms for enhanced parameter estimation on inverted pendulum system dynamics. Mathematics, 12(11): 1625. https://doi.org/10.3390/math12111625

[56] Nappu, M.B., Arief, A., Bansal, R.C. (2014). Transmission management for congested power system: A review of concepts, technical challenges and development of a new methodology. Renewable and Sustainable Energy Reviews, 38: 572-580. https://doi.org/10.1016/j.rser.2014.05.089

[57] Hassan, M.H., Kamel, S., Selim, A., Shaheen, A., Yu, J., El-Sehiemy, R. (2024). Efficient economic operation based on load dispatch of power systems using a leader white shark optimization algorithm. Neural Computing and Applications, 36(18): 10613-10635. https://doi.org/10.1007/s00521-024-09612-2

[58] Bienstock, D., Chertkov, M., Harnett, S. (2014). Chance-constrained optimal power flow: Risk-aware network control under uncertainty. Siam Review, 56(3): 461-495. https://doi.org/10.1137/130910312

[59] Alsac, O., Stott, B. (2007). Optimal load flow with steady-state security. IEEE Transactions on Power Apparatus and Systems, 3: 745-751. https://doi.org/10.1109/TPAS.1974.293972

[60] Christie, R.D. (1993). Power Systems Test Case Archive. University of Washington. http://labs.ece.uw.edu/pstca/dyn30/pg_tcadyn30.htm.

[61] Christie, R.D., Wollenberg, B.F., Wangensteen, I. (2002). Transmission management in the deregulated environment. Proceedings of the IEEE, 88(2): 170-195. https://doi.org/10.1109/5.823997

[62] Zimmerman, R.D., Murillo-Sánchez, C.E., Thomas, R.J. (2010). MATPOWER: Steady-state operations, planning, and analysis tools for power systems research and education. IEEE Transactions on Power Systems, 26(1): 12-19. https://doi.org/10.1109/TPWRS.2010.2051168

[63] Glavic, M., Van Cutsem, T. (2009). Wide-area detection of voltage instability from synchronized phasor measurements. Part I: Principle. IEEE Transactions on Power Systems, 24(3): 1408-1416. https://doi.org/10.1109/TPWRS.2009.2023275

[64] Fischer, M.T., Keim, D.A. (2021). Towards a survey of visualization methods for power grids. arXiv preprint arXiv:2106.04661. https://doi.org/10.48550/arXiv.2106.04661

[65] Ritschel, T.K., Weiß, F., Baumann, M., Grundel, S. (2020). Nonlinear model reduction of dynamical power grid models using quadratization and balanced truncation. at-Automatisierungstechnik, 68(12): 1022-1034. https://doi.org/10.1515/auto-2020-0070

[66] MathWorks. (2023). MATLAB R2023b Documentation. Natick, MA: The MathWorks, Inc. https://www.mathworks.com/help/matlab/.

[67] Milano, F. (2005). An open source power system analysis toolbox. IEEE Transactions on Power Systems, 20(3): 1199-1206. https://doi.org/10.1109/TPWRS.2005.851911

[68] Peng, R.D. (2011). Reproducible research in computational science. Science, 334(6060): 1226-1227. https://doi.org/10.1126/science.1213847

[69] Althof, M. (2022). Benchmarks for the formal verification of power systems. EPiC Series in Computing, 90: 26-43. https://mediatum.ub.tum.de/doc/1696138/l9lqsldr5d96hk0b33m8zb381.Althoff-2022-ARCH.pdf.

[70] Kundur, P. (1994). Power System Stability and Control. New York, NY: McGraw-Hill, Inc.

[71] Xie, Y., Stodden, V., Leisch, F., Peng, R.D. (2014). Implementing Reproducible Computational Research. Boca Raton: Chapman and Hall/CRC.

[72] Happ, H.H. (2006). Optimal power dispatch꞉A comprehensive survey. IEEE Transactions on Power Apparatus and Systems, 96(3): 841-854. https://doi.org/10.1109/T-PAS.1977.32397

[73] Shahidehpour, M., Yamin, H., Li, Z. (2002). Market Operations in Electric Power Systems: Forecasting, Scheduling, and Risk Management. John Wiley & Sons.

[74] Stott, B., Alsac, O. (2007). Fast decoupled load flow. IEEE Transactions on Power Apparatus and Systems, 3: 859-869. https://doi.org/10.1109/TPAS.1974.293985

NOMENCLATURE

KRM	Kron's Reduction Method
IEEE	Institute of Electrical and Electronics Engineers
S1	Stage 1, bus-26 removed
S2	Stage 2, bus-30 removed
S3	Stage 3, bus-29 removed
SCADA	Supervisory Control and Data Acquisition
EMS	Energy Management Systems
DC	Direct Current
MILP	Mixed-Integer Linear Programming
CD	Community Detection
RTS-96	Reliability Test System 1996
V-RMSE	Voltage - Root Mean Square Error
ETAP	Electrical Transient Analyzer Program
KLM	Kron's Loss Model
OPF	Optimal Power Flow
ED	Economic Dispatch
GA	Genetic Algorithms
PSO	Particle Swarm Optimization
DE	Differential Evolution
PSAT	Power System Analysis Toolbox
MATLAB	Matrix Laboratory

CPU	Central Processing Unit
GB	Giga Byte
RAM	Random Access Memory
OS	Operating System
PES	Power and Energy Society
MVA	Mega Volt Ampere
AGC	Automatic Generation Control
NERC	North American Electric Reliability Corporation
IEC	International Electrotechnical Commission